Appendix 1　Histograms and Cumulative Frequency Curves of Cell Average Values

Appendix 2　Flow Charts of Chemical Analysis

Appendix 3　List of Existing Data

Appendix 1 Histogram and Cumulative Frequency Curves of Cell Average Values

(Southern Sierra Madre 1)

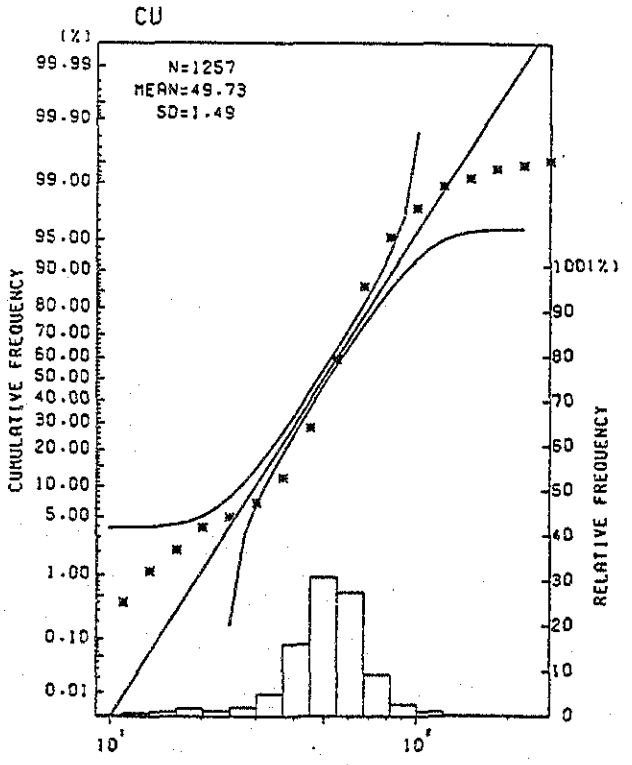

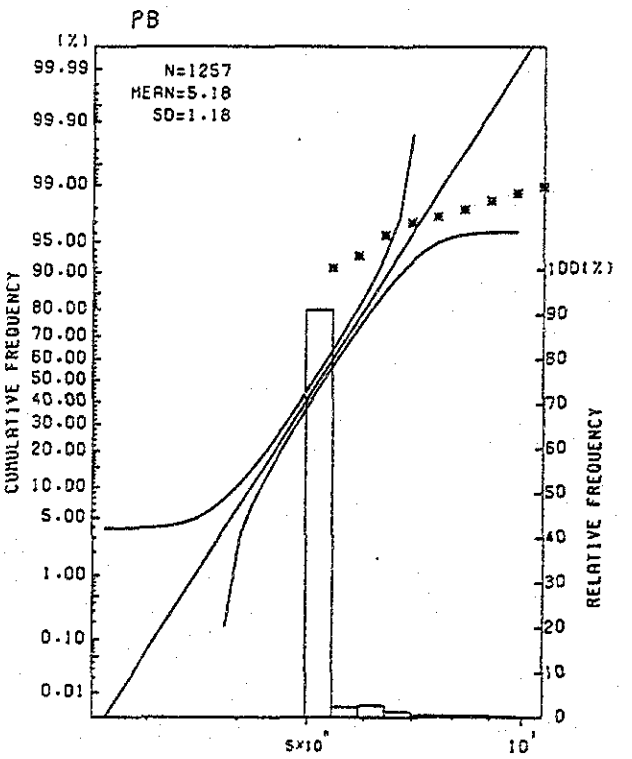

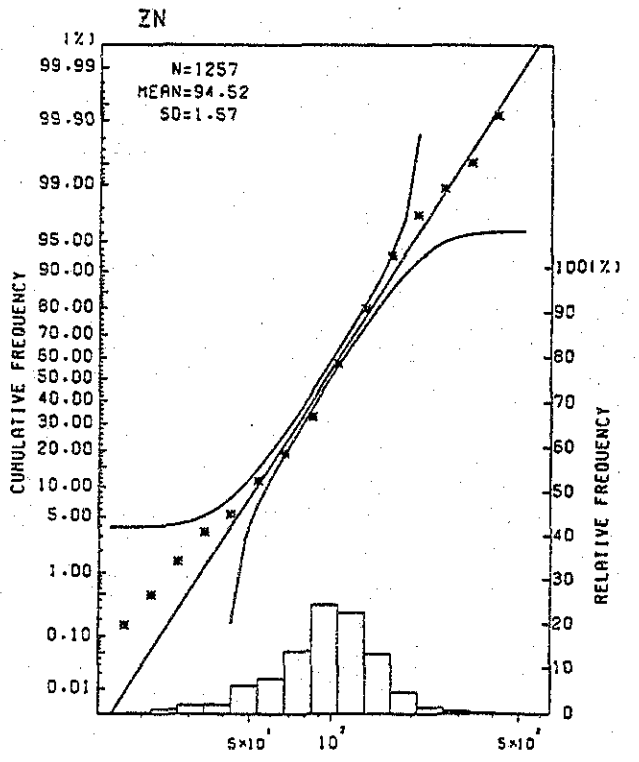

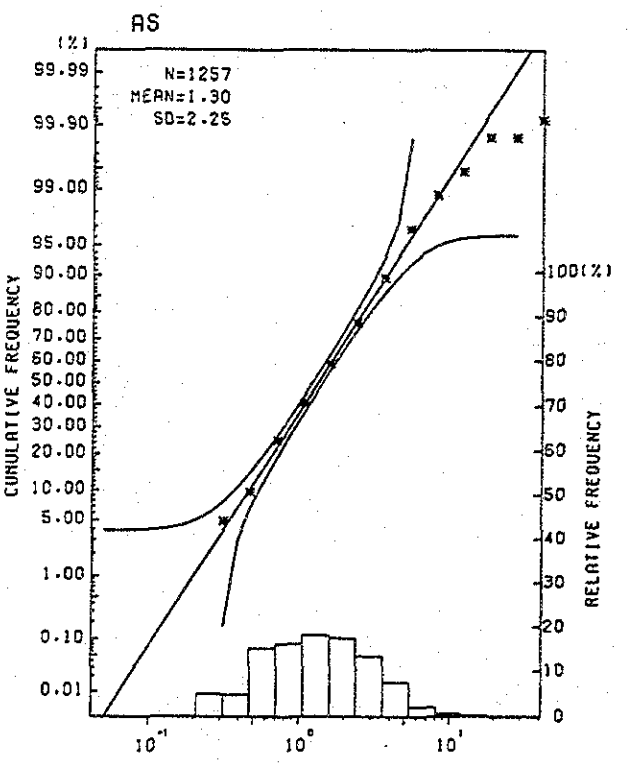

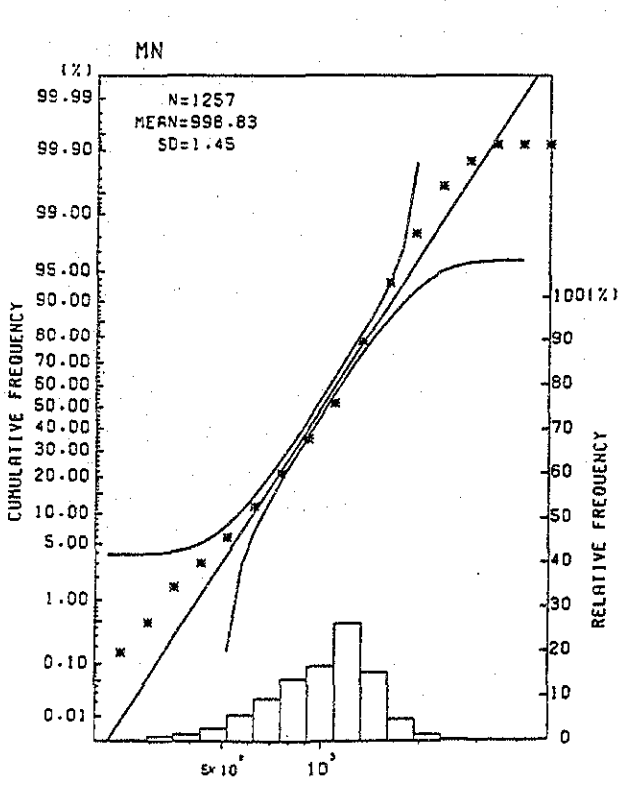

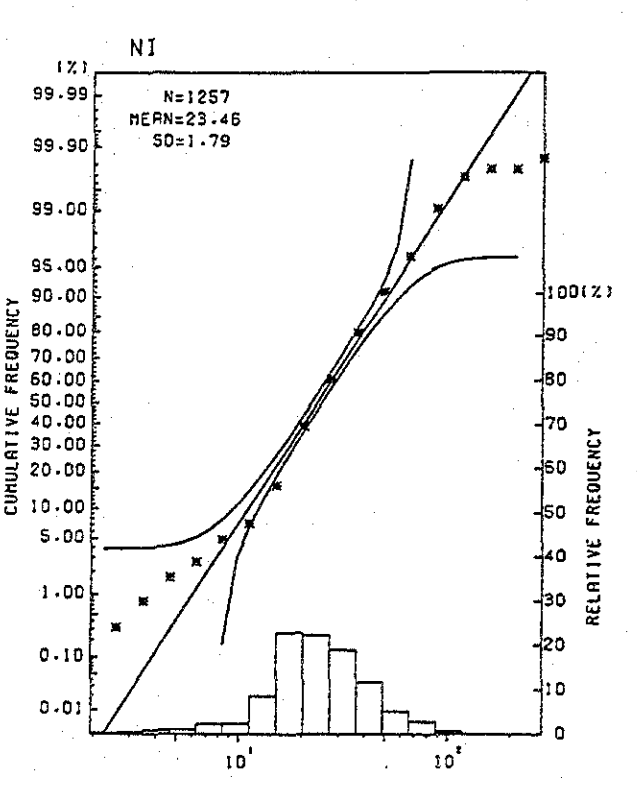

Appendix 1 Histogram and Cumulative Frequency Curves of Cell Average Values

(Southern Sierra Madre 2)

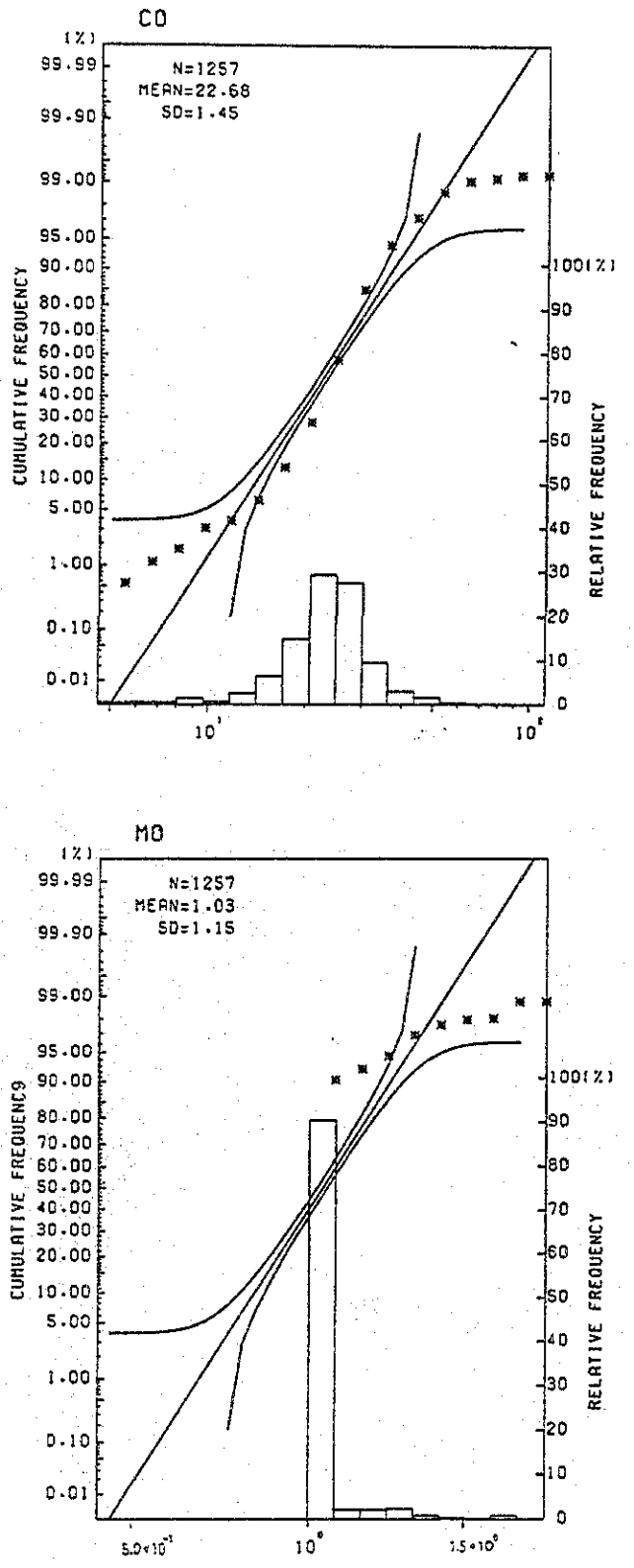

Appendix 2 Flow Charts of Chemical Analysis

Appendix 2-1

Analytical flow chart for Cu, Pb, Zn, Co, Ni and Mn

(A) Digestion Procedure with aqua regina

Sample 1 g.

→ Transfer to the test tube (18×150 mm) Setting test tube stand

← HNO_3 1 ml

← HCl 3 ml

Leave standing One overnight

Boil gently The test tubes are set with aluminum holder on hot plates for 30 min. at 120°C and are occasionally mixed.

← Add approximately 10 ml of distilled water.

Cooling

Setting the volume up to 20 ml. With distilled water.
(Sample solution digested with aqua regina.)

(B) Measurement of contents of Cu, Pb, Zn, Co, Ni and Mn

Sample Solution Digested with aqua regina.

Measurement By Atomic Absorption (AAS).

Element	Flame	Wave Length (Å)
Cu	Air-C_2H_2	3247
Pb	id	2170
Zn	id	2137
Co	id	2407
Ni	id	2320
Mn	id	4033

Appendix 2-2

Analytical flow chart of As, Sb and Hg

(A) Measurement of Sb content

Sample Solution Digested with aqua regina.

Pipet 1 ml.

→ Transfer to the plastic vial

→ Solution (10% KI + 5% ascorbic acid) 0.5 ml

→ 6M-HCl 1 ml.

Hydride generating attachment
0.6% $NaBH_4$ solution

Measurement by Hydration-AAS

Wavelength 2176 Å

(B) Measurement of As content.

Sample Solution Digested with aqua regina.

Pipet 1 ml.

→ Transfer to the plastic vial

→ Solution (10% KI + 5% ascorbic acid) 0.5 ml

→ 6M-HCl 1 ml.

Hydride generating attachment
0.6% $NaBH_4$ solution

Measurement by Hydration-AAS

Wavelength 1974 Å

(C) Measurement of Hg content.

Sample Solution Digested with aqua regina.

Pipet 5 ml.

→ Transfer to the 250 ml. Erlenmayer flask.

→ $(1+1)H_2SO_4$ 5 ml.

→ Distilled water to approximate 100 ml.

→ 6% $SnCl_2$ 1 ml.

Measurement by Reduction vapor-AAS.

(Mercury analyser)
Wave length: 2537 Å

Appendix 2-3

Analytical flow chart of Au, Ag and Ga.

(A) Decomposition of sample.

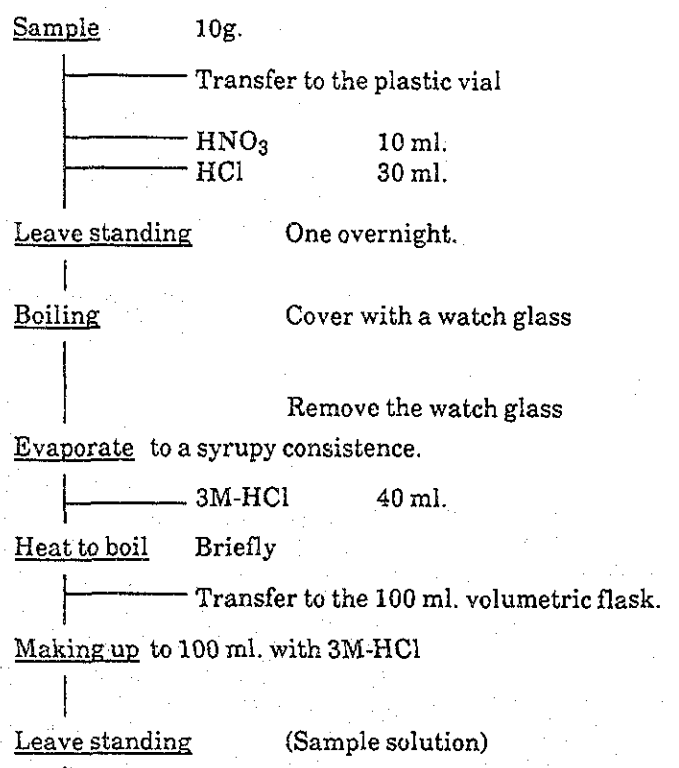

(B) Measurement of Au content.

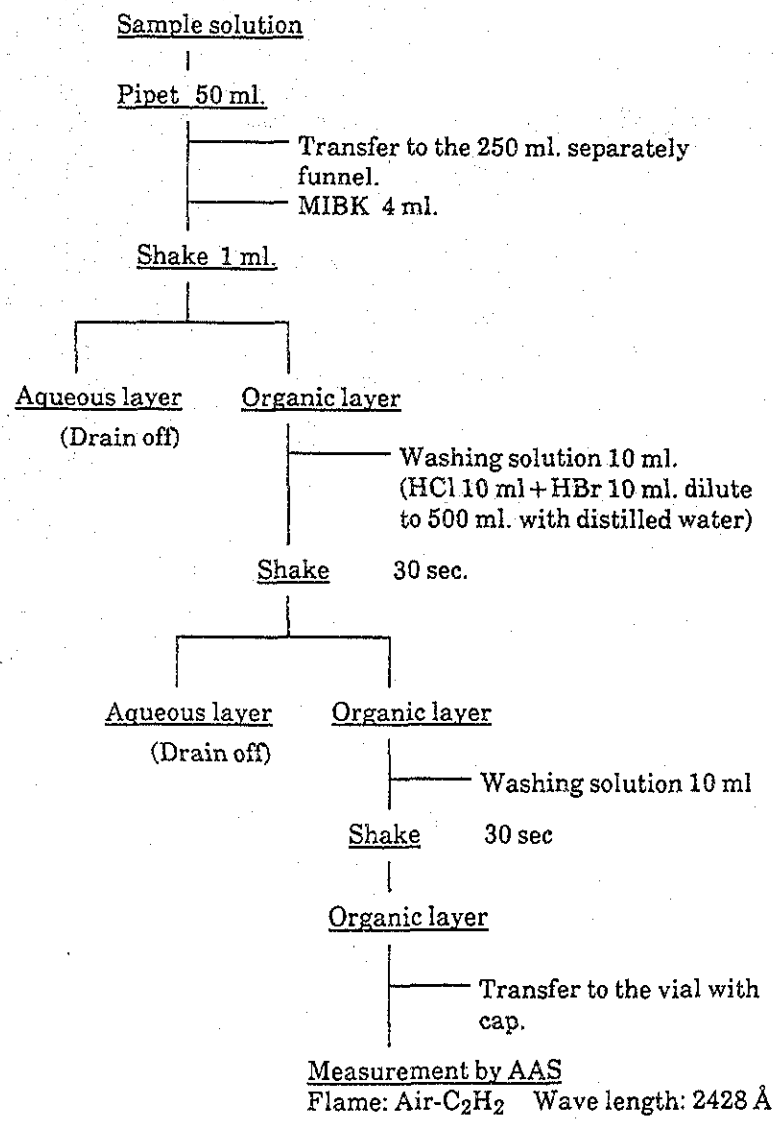

(C) Measurement of Ag and Ga content.

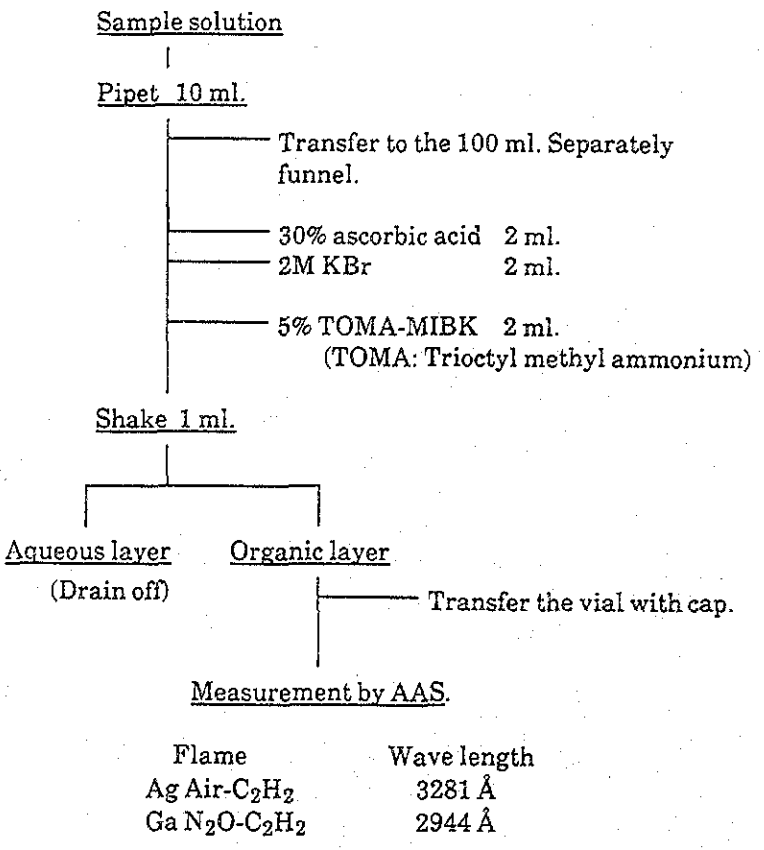

Flame	Wave length
Ag Air-C_2H_2	3281 Å
Ga N_2O-C_2H_2	2944 Å

Appendix 2-4

Analytical flow chart of Cr and W.

(A) Measurement of Cr content.

Sample 0.05 g

- Transfer to the bolosilicate test tube calibrated for 20 ml.
- $KHSO_4$ 0.5 g.

Fusion — Bunsen burner for 5 min. after all sample is dissolved in the melt.

Cooling — Place the test tube on a tray and roll it to spread the melt on the test tube walls. (This facilitates solubilization)

- (1+1)HCl 5 ml. Place the test tube in a hotwater bath.

Heat to dissolved

Making volume up to 20 ml. with distilled water.

Measure by AAS.

Flame: Air-C_2H_2 Wave length: 3579 Å
(Using a strongly oxidizing flame)

(B) Measurement of W content.

Sample 0.25 g

- Transfer to the bolosilicate test tube
- $KHSO_4$ 1 g.

Fusion — Bunsen burner for 5 min. after a quiescent melt has been obtained.

Cooling — Roll the test tube while cooling on a tray.

- HCl 5 ml. Place the test tube in a hot waterbath.

Heat to dissolve

Pipet 4 ml.

- Transfer to another test tube containing 5 ml. of 10% SnCl solution

Heat — Place the test tube in the boiling bath for 10 min.

- 0.6% Zn-dithiol solution 1 ml.

Heat continue for another 10 min. occasionally shaking.

Cooling in cold water

- Petroleum spirit 0.5 ml.

Shake 30 sec.

Compare blue color with standard reference solution.

Appendix 3 List of the Existing Data

NUEVA ECIJA

	REPORT NO.		AUTHOR/S	DATE	TITLE OF REPORTS
*	948	(1358)	M. Liggayu	1970,	Geological investigation of the Gapan Mining Ass. copper prospects in Balintingon, General Tinio, Nueva Ecija
*	953	(1366)	J. Fernandez	1970,	Geological investigation of the Ruby, Buna, Starcom and Ortegon copper prospects, Liggayu, Galbaldon, Nueva Ecija
*	1096	(1569)	A. Paderes	1971,	Report on the geological investigation of Balao, the Villarosa Mining prospects at San Miguel, Bulacan and General Tinio, Nueva Ecija
	1192	(1719)	A. Baptista	1972,	Verification of copper sulfide mineralization at Balintingon, General Tinio, Nueva Ecija
*	1369		D. Abiog	1970,	Geology of portion of Eastern Sierra Madre Range in Quezon and Nueva Ecija Provinces

RIZAL

	REPORT NO.		AUTHOR/S	DATE	TITLE OF REPORTS
	499	(766)	A. Magpantay	1965,	Geologic Investigation of Proposed Cement Plant Site at Daraitan-Nilubugan Area, Tanay, Rizal
*	625		A. Cruz E. Cusi	1966,	Geologic Investigation of the Four Sidling Placer Claims and Vicinity, Antipolo-Teresa Area Rizal for Cement Raw Materials
	726		J.U. Santiago	1964,	Geologic Investigation of the Puray mineral deposits, Montalban, Rizal
*	741	(1084)	C. Llave	1968,	Geological Investigation of Argillaceous Materials in Bos. Antipagak and Abuyod. Antipolo, Rizal for Island Cement Corporation
	759		C.P. Jongco	1965,	Report on the ore reserve estimation of Sta. Ines Mines
*	867	(1245)	A. Cruz	1971,	Geological Investigation of Placer Claims in Tanay, Rizal for Marble
*	1199	(1730)	C. Velasquez	1972,	Geological Verification of Limestone Deposits in the Mining Claims of Pasig Mining Associations in Teresa and Antipolo, Rizal
*	1378	(2067)	C. Llave	1973,	Mineral and Lease Survey Verification of "Francisco" Mining Claim in itio Puting Bato, Barrio Cabuayahan, Teresa, Rizal

BULACAN

	REPORT NO.		AUTHOR/S	DATE	TITLE OF REPORTS
*	229		Crispin, Ganzon Puzon, Malicdem	1957,	Report on the Geologicakl Investigation of Gold-Titanium-Iron Placer Deposit at Sta. Maria, Bulacan
*	501		C. Llave N. Biscocho	1965,	Report on the Geological Investigation of Limestone Deposit in Sitio Suga, Norzagaray, Bulacan
*	527		D. Abiog		Geology of Bulacan Iron Deposits
*	835	(1205)	A. Gorriceta	1969,	Memo Report on the Geological Investigation of the Silica Deposits in Bo. Bayabas, Norzagaray, Bulacan
	921	(1323)	C. Velasquez	1969,	Memo Report on the Geological Investigation & Verification of Placer Mining Claim "Peping of Continental Marble Corp. im Matictic and Bayabas, Norzagaray, Bulacan
	1006	(1434)	C. Velasquez	1970,	Memo Report on the Geological Investigation and Verification of Placer Mining Claims Union Mining Ass., Dulong Bayan, San Jose Del Monte, Bulacan
	1088	(1547)	M. Jandumon	1971,	Report on the Geological Investigation of the Marble Deposits in Sitio Cogonan, Barrio Sibul San Miguel, Bulacan
	1108	(1578)	C.A. Llave	1971,	Geological Investigation of the Lot of Mr. Fidel P. Villafuerte for Siliceous and Clay Materials in Barrio Akle, San Rafael, Bulacan
*	1293	(1918)	P.H. Liñgat	1973,	Geological and Mineral Verification of Aliw III Placer Claim in Sitio Pulong Bato, Barrio Alagao, San Ildefonso, Bulacan
*	1394		A.J. Gorriceta	1973,	Geological Verification of Clay Deposits in Barrio Camachino, San Ildefonso, Bulacan
*	1440		C.A. Llave	1974,	Mineral & Survey Verification of Emerald & Diamond Placer Mining Claims in Bo. Camachille, Angat, Bulacan

BULACAN

REPORT NO.		AUTHOR/S	DATE	TITLE OF REPORTS
* 1456		P.H. Liñgat	1974,	Report on the Geological & Meneral Verification of "Don Paco" Placer Claim for Gypsum in Sitio Suklay, Bo. Sibul Spring San Miguel, Bulacan
* 1498		C.A. Llave	1974,	Mineral Verification of Violita VIII Mining Claim in Bo. Camachin, San Miguel Bulacan
1521		E.M. Manalang	1975,	Mineral Verification of the Gold-Iron-Titanium Placer Deposit Along Sta. Maria River and San Jose Del Monte Mun., Prov. Bulacan
* 1582	(1975)	H.P. Quiazon	1975,	Memorandum Report on the Gas Emanation at Bo. Balaong, San Miguel, Bulacan

QUEZON

REPORT NO.		AUTHOR/S	DATE	TITLE OF REPORTS
* 187		V. de los Santos D. Abiog	1956,	Report on the geological investigation of coal claims in Anibauan, Burdeos (Polillo Island) Quezon for the Commonwealth Ceramics Corp.
* 207		I. Antonio		Report on the survey of the Polillo Forest reserve
* 475		D. Abiog J. Mantaring	1964,	Geologic investigation of gold-zinc prospect in Angelo Mountains, Infanta, Quezon
* 514 306		O. Crispin M. Pacis	1959,	Memo report on the preliminary geologic investigation of copper prospects in Ibuna-Agosis area, Dingalan, Quezon Province
* 553	(1001)	J. Fernandez O. Abarquez B. Vera Cruz P. Estupugan	1967,	Geology of Polillo Iron prospects, Quezon
* 682		J. Fernandez B. Vera Cruz P. Estupigan O. Abarquez	1967,	Preliminary report on the regional geology of Polillo Island group, Quezon
* 738	(1075)	A. Cruz D. Abiog	1967,	Geologic investigation of the Placer claims of Umiray Mng. Co., in Dingalan, Quezon for cement raw materials location of plant site
* 761	(1107)	C. Llave R. de Luna	1968,	Report on the geological investigation of limestone deposit in sitios Pangasinan and Tingtingon, Bo. Cabungalunan, Burdeos, Quezon
* 769		V. delos Santos F.D. Spencer	1957,	Geology and coal resources of central Polillo Island, Quezon
* 816		GSD	1968,	Mineral deposits of Infanta and Polillo Island, Quezon
* 829	(1193)	D. Abiog	1969,	Geologic investigation of cement raw materials deposits in Dingalan, Quezon
* 1043	(1488)	A. Curz	1970,	Memo report on the geologic investigation of mineral claims of Phil. Mineral Industries Chemical Pioneer Corp. in sitio Pandayan, Umiray, General Nakar, Quezon
* 1212	(1704)	A. Cruz	1972,	Marble in Southern Dingalan, Quezon
* 1434		C.V. Ramos	1974,	Geological verification covering 38 lode claims of the Lumbay copper deposit in Limutan, General Nakar, Quezon
* 1567	(1975)	M.G. Pacis	1975,	Mineral verification of Three areas applied for exploration permit at Umiray Forest Reserve General Nakar, Quezon province
* 1648	(1976)	P. Estupigan	1976,	Mineral and geological verification inside the Umiray Forest reservation at Bo. Lumbay General Nakar, Quezon the exploration permit application
* PG-Q2-1		D.G. Malicdem	1975,	Notes on the geology and exploration of Collosal-Lepanto Copper Project, Gen. Nakar, Quezon, Journal of GSP. Vol. 29, No. 1, March 1975
* Q-376		R.E. Yumul	1977,	Inspection and verification of the exploration activities of Marcopper Mining Corporation, covered by Exploration permit No. 50 w/in a portion of the umiray forest reservation at BO. Lumbay, Gen. Nakar, Quezon
* Q-1		R.J. Robles	1980,	Progress report on the detailed geological mapping and geochemical sampling of Matani area, Gen. Nakar, Quezon, for April 1980
* Q-2		E.R. Malaca	1982,	Individual accomplishment report on the detailed geological mapping of Limutan-Irramang area, Gen Nakar, Quezon
* Q-240		A. Cruz	1970,	Memorandum report on the geological investigation of mineral claims of Philippine Mineral Industrial Chemical Pioneer Corporation in Sitio, Pandayan, Umiray, Gen. Naker, Quezon

Consolidated Report on Samar, Leyte and Dinagat · Siargao Areas

SUMMARY

A total area of 8,289 km^2 in Leyte, Dinagat and Siargao was covered by geological and geochemical prospecting in 1986 as a part of "The Mineral Exploration, Mineral Deposits and Tectonics of Two Contrasting Geologic Environments in the Republic of the Philippines" project.

The results were statistically processed and evaluated taking into considerations both local and regional geological perspectives, utilizing in the process all the relevant available results from the present geological survey and mineral prospecting in addition to the existing geoscientific data about the area.

The study area is located in the eastern portion of the Philippine Mobile Belt. The tectonics and structural configurations of the study area are intensely influenced and related to movements associated with the left-lateral Philippine Fault and the westward subduction of the Philippine Sea Plate along the Philippine Trench.

The survey area is devided into three zones by geological characteristics: Leyte, Dinagat-Sargao and Masapelid zones.

In Leyte, the basement unit consists mainly of Mesozoic crystalline schist which is almost always covered by post-Tertiary sedimentary and pyroclastic rocks except in the northeastern and southwestern part of the island. The Dinagat - Siargao area, on the other hand, is characterized by a Cretaceous ophiolite basement unit which is exposed over 70% portion of the are. It is partially covered by Eocene pyroclastic rocks in Dinagat while Miocene to Pleistocene limestones overlie the ophiolite in Siargao and Bucas Grande. Masapelid Island is composed of Miocene basaltic to andesitic lavas and sedimentary rocks.

The main igneous activities in Leyte were the Eocene and Oligocene diorite intrusions, Middle Miocene andesite and basalt eruptions and the Pleistocene andesite extrusions. No igneous rocks were encountered in Dinagat and Siargao except for the Cretaceous ophiolite basement.

The field surveys conducted led to the recognition of several types of mineralization in the study area. In Leyte, cupriferous massive sulfide, copper veins later enriched in gold by late-stage mineralizing fluids, nickeliferous veins and residual type manganese concentrations were observed. Chromite orthomagmatic mineralization associated with the ophiolite complex and auriferous quartz veins were encountered in Dinagat and Siargao.

The regional analyses and interpretations of the geochemical anomalies defined by the ten (10) selected elements were carried out for three assigned populations namely Samar, Leyte and Dinagat - Siargao. The selected elements utilized in the study of the Samar and Dinagat - Siargao geochemical samples are Cu, Pb, Zn, Ag, As, Mn, Ni, Co, Cr, Hg. The same group of elements were analysed for the Leyte geochemical samples except for Cr which was not analysed but replaced by Mo. Only univariate analysis was carried out for the Samar area since the sample density of this area was small as compared to the other areas.

The whole survey area was divided into 2 km × 2 km cells. Four types of statistical analyses were then carried out using the geometric means of each of the elements found in each cell. The four types of statistical analyses utilized were:

1. Univariate analyses of cell average values;
2. Univariate analyses of moving average values which determine the average value of nine cells that correspond to the value of the central cell;
3. Univariate analyses of high-pass filter value which is the positive difference between each cell average and the moving average value;
4. Multivariate analyses (Factor Analyses) for the cell average values. The results are shown in 1 : 1,000,000 scale maps (Attached Pl. 2-1 to Pl. 2-4);

The geological significance of the statistical results were then evaluated utilizing the data on the distribution of igneous bodies, geological structures and observed alteration patterns associated with the inferred mineralization types.

Finally, three localities each from Leyte and Dinagat - Siargao were selected as promising and warranting further study and prospecting. The localities are prioritized from I to III (Attached Pl. 10).

Leyte Area

I. The northeast coast of Panaon Island in southern Leyte: This zone, where the Anilao mineral showing can be found, is characterized by overlapping geochemical anomalies in the Central Highland Volcanics.
The assumed type of mineralization and associated commodites; Vein type mineralization, Au and Ag.

II. The northern portion of Sogod in southern Leyte: This zone is also characterized by overlapping geochemical anomalies in the Central Highland Volcanics. The Sogod mineral showing is located in this zone.
The assumed type of mineralization and associated commodities; Vein type mineralization, Cu, Pb and Zn.

III. The northwestern side of Tacloban in northeastern Leyte: This zone corresponds to an area characterized by overlapping geochemical anomalies in a Cretaceous ophiolite. Curajo, Caibaan, Suhi and other mineral showings are encountered in this zone.
The assumed mineralization types and associated commodities; Vein type mineralization, Cu and Zn.

Dinagat - Siargao Area

I. Northern part of Masapelid Island: This zone is characterized by overlapping geochemical anomalies in Miocene altered andesites and their immediate vicinity. The Cangmod mineral showing belongs to this zone.

The assumed mineralization type and associated commodities; Auriferous quartz vein type mineralization, Au and Ag.

II. The vicinity of Mt. Gaboc in the southern Dinagat Island: This zone is characterized by overlapping geochemical anomalies. Although no mineral showing has been encoutered, the locality is very close to the Nonoc nickeliferous laterite mine.
The assumed mineralization type and associated commodities; Nickeliferous laterite type concentration, Ni and Cr.

The Mineral Exploration-Mineral Deposits and Tectonics of two Contrasting Geologic Environments in The Republic of The Philippines

Consolidated Report on Samar · Leyte · Dinagat · Siargao Area

Contents

List of Figures

List of Tables

List of Attached Plates

Pl.1 Geological Map and Section (1:1,000,000)

Pl.2-1 (No. 1 to No. 11)
Geochemical Analysis Cell Average Values Distribution Map (1:1,000,000)

Pl.2-2 (No. 1 to No. 11)
Geochemical Analysis Moving Average Values Distribution Map (1:1,000,000)

Pl.2-3 (No. 1 to No. 10)
Geochemical Analysis High-pass Filter Values Distribution Map (1:1,000,000)

Pl.2-4 (No. 1 to No. 5)
Geochemical Analysis Factor Analytical Values Distribution Map (1:1,000,000)

Pl.3 Distribution Map of Anomalous Values in Panned Samples (1:1,000,000)

Pl.4 Distribution Map of the Major Heavy Minerals Wt % in Panned Samples (1:1,000,000)

Pl.5 Compiled Gravimetric Map (Bouguer Anomalies) (1:1,000,000)

Pl.6 Compiled Aeromagnetic Map (1:1,000,000)

Pl.7 Lineaments Map (LANDSAT Images) (1:1,000,000)

Pl.8 Locality Map of Mineral Showings (1:1,000,000)
Attached Index Table of Mineral Showings

Pl.9 Index Map of Existing Data regarding Survey Works of the Area (1:1,000,000)

Pl.10 Relation Map between Promising Area and Mineral Showings Localities (1:1,000,000)

Appendixes

Appendix 1 Histograms and Cumulative Frequency Curves of Cell Average Values

Appendix 2 Flow Charts of Chemical Analysis

Appendix 3 List of the Existing Data

1. Introduction

1-1 Purpose and Scope

1-1-1 Background and Scope

Pursuant to the Implementing Arrangement (I/A) entered into between the Government of Japan through the Japan International Cooperation Agency (JICA) and the Metal Mining Agency of Japan (MMAJ) and the Government of the Philippines through the Mines and Geo-Sciences Bureau (MGB) on September 26, 1984, a project, officially titled "The Mineral Exploration-Mineral Deposits and Tectonics of Two Contrasting Geologic Environments" was carried out in the Republic of the Philippines.

This report embodies results of the synthetic evaluation on the area of Samar, Leyte and Dinagat-Siargao which are included in the above mentioned project. The field survey took place from in August to November, 1985 in Leyte and Dinagat-Siargao and, from July to August, 1987 in parts of Samar respectively.

1-1-2 Objectives of the Report

This report embodies the summary of the results of the survey and study of the existing data regarding the mineral resources in the Samar, Leyte and Dinagat-Siargao areas which are located in the eastern part of the Republic of Philippines.

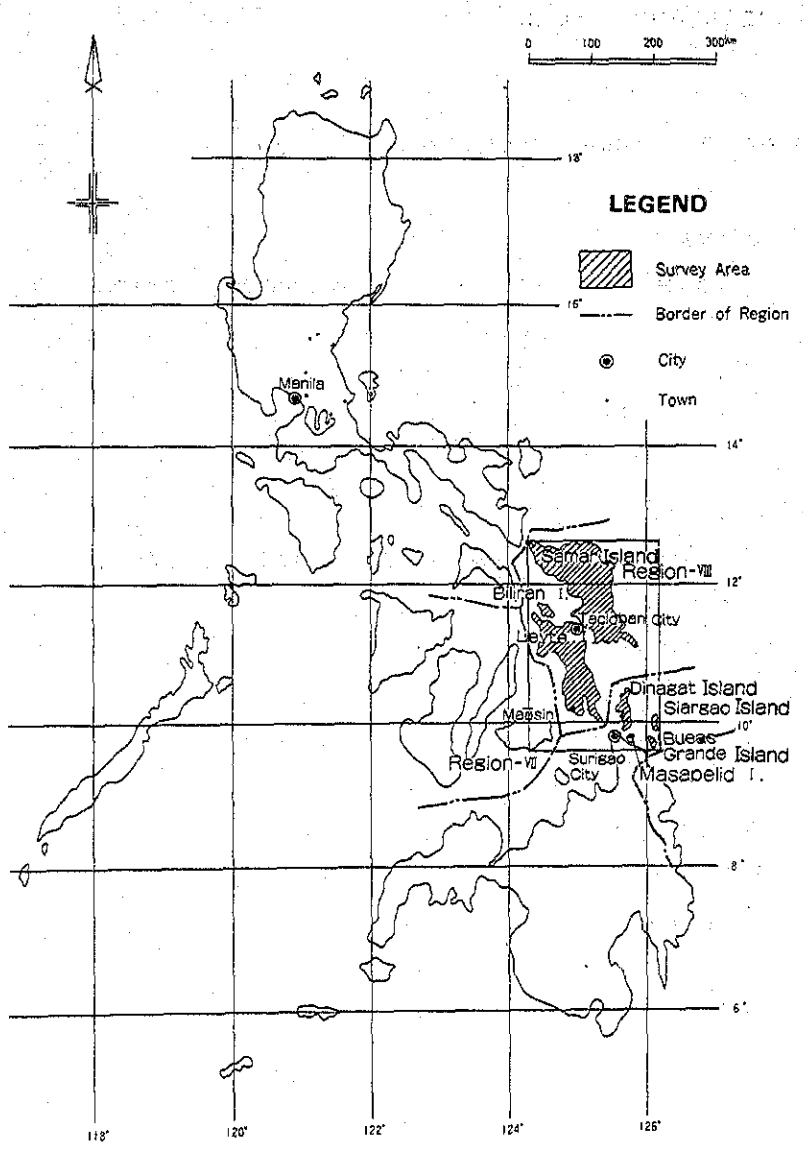

Fig.-1 Survey Area

The objectives of this report include the recognition and derivation of the mineral resources distribution in the different survey areas, correlation, processing and analysis of all acquired data to come up with an evaluation of the mineral potential.

1-2 Regional Setting

1-2-1 Location

The survey area is located at the eastern side of the Visayas of the Republic of the Philippines. It lies within the geographical coordinates of lat. 9°33' to 12°45'N, and long. 124°15' to 126°11'E, and is composed of Samar, Leyte (including Biliran Is. and Panaon Is.) and Dinagat-Siargao (including Bucas Grande Is. and Masapelid Is.).

In terms of administrative regions, Samar and Leyte belong to Region VIII while Dinagat-Siargao belong to Region X.

Total survey area covers 10,437 km^2. The highest peak in Samar is Mt. Capoti-An (670 m), that of Leyte is Mt. Lobi (1,350 m) and that of Dinagat is Mt. Redondo (929 m).

1-2-2 Access

Tacloban City is the provincial capital of Leyte, and is located about 650 km SE of Manila. There are regular flights from Manila to Tacloban City. Commercial shipping is also available either from Manila and Cebu City. No. 1 National Highway from Manila via Samar to Liloan in Southern Leyte is available. Ship service from Surigao in Northern Mindanao to Dinagat and Siargao Is. is also available.

1-2-3 Climate

The survey area belongs to the Western Pacific Monsoon Climate zone. Western Leyte has even rainfall throughout the year, while Samar, Eastern Leyte and Dinagat-Siargao Is. have almost no dry season and October to March usually have the highest rainfall. Annual average temperature is 27°C and annual precipitation ranges from 1,900 mm (Maasin, Southern Leyte) to 3,600 mm (Dinagat). The Pacific Ocean side of the area is a part of Philippine Typhoon belt which is usually ravaged by typhoons in the latter half of the year.

1-2-4 Vegetation and Others

At the lowland along coasts, mangrove grow abundantly in each island. Coastal plains and riversides are planted with rice. The alluvial plane in Northeastern Leyte is the major producer of these crops. The inland portions of each island are usually covered by virgin forest although some places are bare as a result of indiscriminate logging.

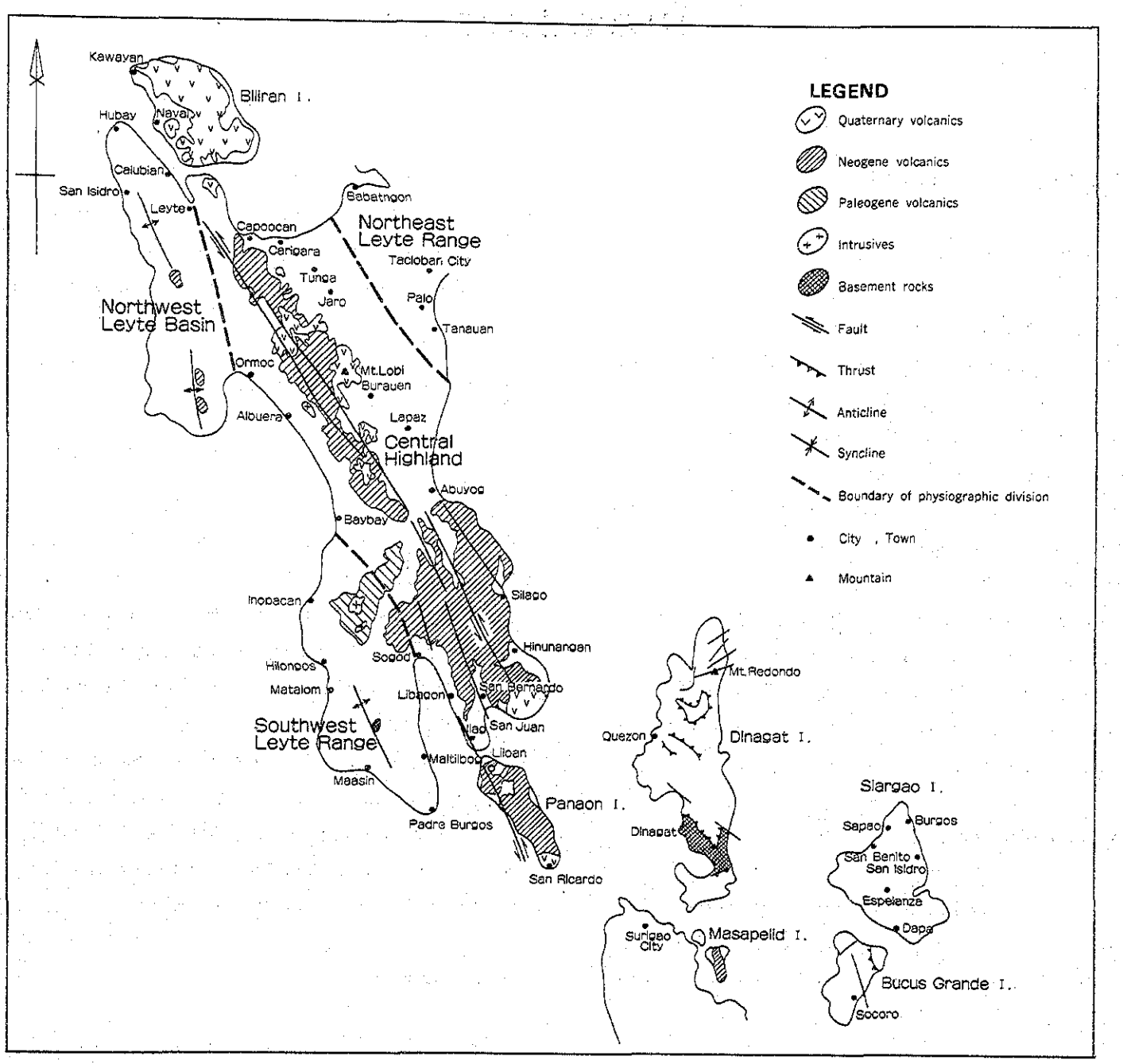

Fig. -2 Tectonic Division of Leyte, Dinagat and Siargao Area

1-3 Member of the Survey Team

1-3-1 Planning and Negotiation

Japanese Panel

H. Shinokawa	Ministry of International Trade and Industry (MITI)
M. Aoyama	id.
H. Kainuma	Japan International Cooperation Agency (JICA)
H. Hirano	Metal Mining Agency of Japan (MMAJ)
N. Sato	id.

Philippine Panel

R.D. San Juan	Department of Environment and Natural Resources (DENR)
P. C. Caleon	Mines and Geo-Sciences Bureau (MGB)
R.M. Luis	id.
R. L. Almeda	id.
A. Apostol Jr.	id.

1-3-2 Preparation of the Consolidated Report

Japanese Panel

Y. Okubo	Overseas Mineral Resources Development Co., Ltd. (OMRD)
Y. Uehara	id.
Y. Shimazaki	id.

Philippine Panel

R.M. Samaniego	Mines and Geo-Sciences Bureau (MGB)
M.V. Garcia	id.
B. S. Vargas	id.
R. M. Luis	id.
R. L. Almeda	id.
N.V. Ferrer	id.
A. Apostol Jr.	id.
E. Esguerra	id.
A. Cabantog	id.
V.M. Sunga	id.
U. Palaganas	id.

1-4 Methodology

The analyses and interpretation of the survey data were conducted as follows.

1-4-1 Survey Area

The survey area was divided into three parts for the convenience of geochemical analysis and geological description: Samar, Leyte and Dinagat-Siargao areas. Geological description and divisions were made based on the physiographical features of each area. The Leyte area was divided into the northwestern basin (hereinafter called as NW Leyte or NLB), southwestern Leyte mountains (hereinafter called as SW Leyte or SLR), central highland (hereinafter called as Central Highland or CH) and northeastern mountains (hereinafter called as NE Leyte or NLR). The Dinagat-Siargao area, on the other hand, was divided into Dinagat Island, Siargao Island, Bucas Grande Island and Masapelid Island.

Geochemical analyses were carried out on three populations, namely, Samar, Leyte and Dinagat-Siargao.

Only univariate analyses was carried out on the Samar data. No geological description for Samar is presented as field survey has been suspended since August, 1987.

1-4-2 Stratigraphy

In this report, the stratigraphic classification which has been agreed upon between the Japanese and Philippine panels during the workshop held in Manila in June, 1988 is used. Geological descriptions presented here were adopted from the Leyte (E. Esguerra & A. Cabantog, 1989, ms.) and Dinagat-Siargao (V.S. Sunga & U. Palaganas, 1986, ms.) unpublished reports.

1-4-3 Geochemical Analyses

Geochemical analyses were carried out on three populations, consisting of Samar, Leyte and Dinagat-Siargao.

Anomalous zones were identified through the following process. The whole survey area was divided into 2 km × 2 km cells. Univariate and multivariate analyses of the average values of all the geochemical data of each cell were carried out. Univariate analyses of the moving average values of every nine cells and univariate analyses of the high-pass filter values (the differences between the cell average values and the corresponding moving average values) were also done (as for Samar, multivariate analyses was not carried out, since the geochemical sample density was low compared with the other areas).

A total of 9,630 stream sediment samples from the whole survey area was used for the analyses. The analysed elements include, Cu, Pb, Zn, Ag, As, Mn, Ni, Co, Hg and Cr for Samar, Cu, Pb, Zn, Ag, As, Mn, Ni, Co, Mo and Hg for Leyte and Cu, Pb, Zn, Ag, As, Mn, Ni, Co, Hg and Cr for Dinagat-Siargao.

1-4-4 Heavy Mineral Samples

In addition to the stream sediment samples, 222 heavy mineral samples from Leyte and 118 heavy mineral samples from Dinagat-Siargao were collected by panning and chemically analyzed for Au, Ag and Ga. The data collected were treated by univariate analyses. Thirty samples from Leyte and ten from Dinagat-Siargao were randomly selected and modal analyses of the component minerals were done.

1-4-5 Existing Regional Survey Data

Available data on previous works on the area were compiled in the lineament map, gravity map, aeromagnetic survey map and mineral showings distribution map at a scale of 1:1,000,000 to conform with the geological map (Attached P1-3, 4, 5, 6. Existing survey data list is presented in the Appendix).

1-5 Achievements of the Project

1-5-1 Conclusions

Four main types of mineralization have been recognized in the survey area (Fig. 2 and Pl. 10).

(1) Massive sulphide type mineralization associated with the pillow basalts of the Cretaceous ophiolite located in Northeastern Leyte.
(2) Vein type mineralization mainly fissure fillings, as noted in the Miocene Central Highland Volcanics of Leyte and Mabuhay Andesite of Masapelid Is.
(3) Residual type Ni, Cr and Mn concentration associated with laterized serpentinites and manganese nodules in pyroclastics.
(4) Orthomagmatic type chromite mineralization believed to have originated through magmatic differential processes of the ultramafic rocks in Dinagat Is.

Taking into consideration all the relevant available data, five promising areas are selected with the following priorities.

Leyte area

(I) Northeastern coast of Panaon Is. in Southeastern Leyte.
This area is characterized by overlapping anomalous zones of Cu, Pb, Zn, As and Hg in the Miocene Central Highland Volcanics.
Two mineral showings are known, Pinut-An (intermittently operating) at the southern part and Anilao at the northern part. Gold bearing quartz vein type mineralization and is indicated and the expected commodities are Au and Ag.

(II) Northern part of Sogod in Southern Leyte.
This area is also characterized by overlapping anomalous zones of Cu, Pb, Zn, As and Hg in the Miocene Central Highland Volcanics.

Mineral showing in Sogod is known. Vein type mineralization is indicated and the expected commodities are Cu, Pb and Zn.

(III) Northwestern portion of Tacloban in the northeastern coast of Leyte.
This area has overlapping anomalous zones of Zn, Mn and Co and observed in the Cretaceous Tacloban Ophiolite.
Several mineral showing are known (Curajo, Caibaan and Suhi, etc.). Massive and vein types mineralization is indicated and the expected commodities are Cu, Pb and Zn.)

Dinagat-Siargao area

(I) Northern part of Masapelid Island.
This area exhibits overlapping anomalous zones of Cu, Pb, Zn, As and Hg in the altered Miocene Mabuhay Andesite.
Mineral showing in Cangmod is known. Gold-bearing quartz vein type mineralization is expected and the assumed commodities are Au and Ag.

(II) Vicinity of Mt. Gaboc in southern Dinagat Island.
This area is characterized by overlapping anomalous zone of Mn, Co, Ni, and Cr in the Cretaceous ultramafic rocks.
No mineral showing is known, but its location is very close to Nonoc Mine. Nickeliferous laterite type concentration is indicates (similar to Nonoc Mine) and the expected commodities are Ni and Co.

2. Geology and Mineralization

2-1 Geological Setting (Fig. 2.3. Attached P1.-1)

The survey area is located in the central part of the Philippine Mobile Belt and consists of the Leyte and Dinagat-Siargao areas belonging to the Central Physiographic Province and Eastern Physiographic Province respectively. The former is mostly covered by Quaternary and Tertiary volcanics and sediments deposited either on the pre-Cretaceous metamorphic basement or Cretaceous ophiolite that overrides the metamorphic basement. The Cretaceous ophiolite is widely exposed on the Dinagat-Siargao area.

The Philippine Fault, which is inferred to have commenced movement during Miocene, traverses the central part of the Leyte Island, trending NNW which is nearly parallel to the Philippine Trench.

The structures of this area consequently are dominated by folds trending from NNW to N-S. The Miocene Central Highland Volcanics occur mainly along the Philippine Fault Zone and show NNW elongated forms similar to the trend of the fault zone. It is distributed intermittently in the Leyte Island.
The Pleistocene Quaternary volcanics also show the same features.

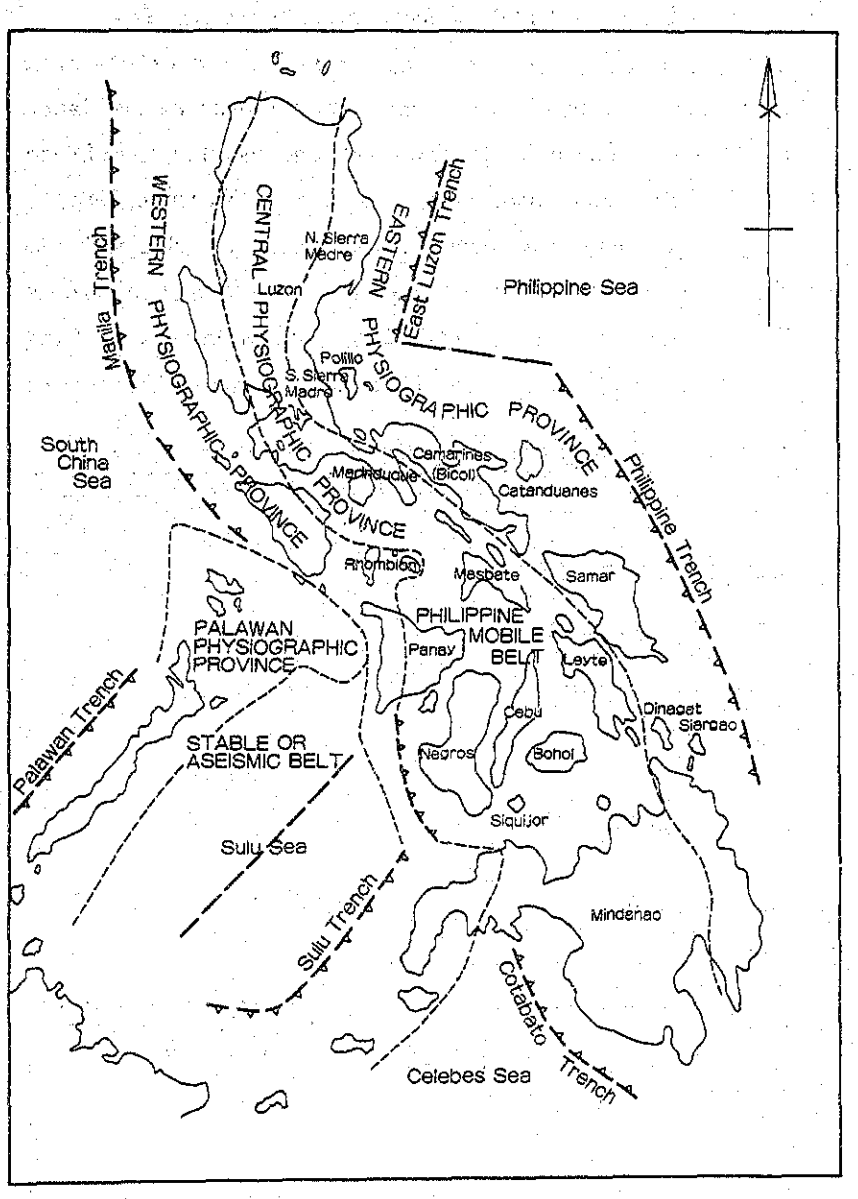

Fig. -3 Major Physiographic Elements in the Philippines (After G.R. Balce et al., 1981)

2-1-1 Leyte Area

The basement rocks of this area, composed of pre-Cretaceous metamorphic rocks (Lawagan Metadiorite and Babatngon Metamorphics), are believed to be the remnants of the primitive crust of the Cebu-Bohol-SW Leyte block. The Cretaceous ophiolites (Malitbog and Tacloban) were thrusted probably during the Eocene over these basement rocks. These older rocks occur only in small patches in Southwest and Northeast Leyte.

Igneous activities associated with the subduction along the Philippine Trench which shifted eastward during the Paleocene have formed the igneous and sedimentary rock units of Tertiary and Quaternary age covering almost the whole Leyte Island.

Regarding the sedimentary rock units of the backarc basin, the Taog Formation, Tagnocot Formation, Kadlum Conglomerate, Calubian Limestone (Miocene), Bata formation (Miocene to Pleistocene) and Hubay Formation (Pliocene - Pleistocene) are exposed in NW Leyte, while the Dacao Formation, Danao Formation (Miocene), Masonting Formation, Pangasgan Formation (Miocene to Pleistocene), and Matalom Formation (Pleistocene) are distributed over the Central Highland to NW Leyte.

The sedimentary rock units of the forearc basin which include the San Jose Formation, San Ricardo Formation (Miocene), and Bagahupi formation (Miocene to Pliocene) are distributed in NE Leyte while the Dolores Formation (Pliocene) mainly occurs in the Central Highland.

Intrusive bodies are the Hindang Diorite (Eocene) and the Albuera Diorite (Oligocene). The major volcanic rock units are the Central Highland Volcanics (Middle Miocene) and Quaternary Volcanics (Pleistocene).

2-1-2 Dinagat-Siargao Area

The oldest rock unit in the area is the Middle Cretaceous Dinagat Ophiolite. This ophiolite is made up of serpentinized hartzburgites, chromite-bearing dunites, isotropic gabbros, diabase dike and pillow basalts. Layered ultramafic units are well defined in the northern parts of Dinagat and Bucas Grande Islands gradually becoming tectonites toward the south. Imbricate faulting, which might be related to the ophiolite emplacement, caused the thrusting of the ultramafic complex over the mafic member of the ophiolite. The Dinagat Ophiolite is thrusted over the Nueva Estrella Amphibolite schist which is exposed as a tectonic window in the southern part of Dinagat Island. The Dinagat Ophiolite as exposed in Dinagat Is. is unconformably overlain by the Eocene Loreto Clastics. In Siargao and Bucas Grande Is., the Miocene to Pleistocene Siargao Formation consisting mainly of interbedded limestone and clastic rocks unconformably overlies the ophiolitic rocks, while in Dinagat Is., it unconformably overlies the Loreto Clastics. Since these islands are composed mainly of ultramafic rocks they have great potentials for chromite deposits and other related minerals.

The rock units of Masapelid Is. consist of Oligocene to Miocene pyroclastics (Bacuag Formation), sedimentary rocks (Masapelid and Timamana Formation) and volcanic rocks (Mabuhay Andesite).

Masapelid Island is lithologically different from those of the above mentioned islands but is somewhat related in terms of its tectonic evolution.

2-2 Stratigraphy

The stratigraphic section agreed upon during the RP-Japan Workshop in June, 1988. are presented in Figures 4, 5, 6, 7, 8, 9 and 10.

2-2-1 Leyte Area

The stratigraphy of Leyte Island presented in accordance to the different physiographic subdivisions are; SLR, NLB, CH and NLR (Fig.-2)

2-2-1-1 Southwest Leyte (SLR) (Fig.-4)

Lewagan Metadiorite is believed to be the pre-Tertiary basement rock of magmatic arc origin. The unit occurs only as a small patch in the central part of SLR and has no direct relationship with the SLR ophiolitic rocks. The present outcrop is unconformably overlain by the Paleocene sedimentary Amontay Formation. The age of the unit is believed to be pre-Cretaceous (Esguerra and Cabantog, ms., 1989).

Malitbog Ophiolite consists of serpentinized harzburgite, minor dunite, cumulate and isotropic gabbro, diabase dike complex and pillow basalts. It occurs as a patch in the central portion of the area. It is inferred to be in thrust contact with the basement metamorphic rocks based on the observations made on other areas of the Cebu-Bohol-Leyte Block.

Tigbauan Formation consists of red chert, red shale, cherty limestone and pelagic limestone and overlies where the Malitbog Ophiolite unconformably. It occurs as a small patch. The age of the formation is probably Pre-Tertiary.

Amontay Sandstone is essentially a Paleocene turbidite sequence deposited unconformably over the Lawagan Metadiorite. The sequence is composed of well-indurated sandstone, siltstone, phyllitic mudstone and marblized limestone. Only one outcrop is observed in the central part of the area.

Gilonon Formation is subdivided into lower, middle and upper portions. The lower unit is composed of basalt-andesite flow breccias. The middle unit consists of turbiditic basaltic wacke, siltstone and green tuff. The upper portion of the formation consists of quartzofeldspatic sandstone and shale. This formation occurs in small patches in the central part of the area. The age of the Gilonon Formation is Late Miocene (Florendo, 1984) and it unconformably overlies the Amontay Sandstone.

Dacao Formation consist of steeply dipping sandstone and siltstone with occasional interbeds of conglomerate and minor volcanic flow. It overlies the Gilonon Formation unconformably and occurs in an intermittent N-S trend in the central part of the area. The age of the formation is inferred to be Early Miocene (Florendo, 1984).

Danao limestone is massive, coralline-algal type limestone and is a shallow marine deposit. It occurs extensively in the northern and central parts of the area and in the mountain part of the Central Highland. The formation overlies the Dacao Formation unconformably and is Middle Miocene in age (Florendo, 1984.).

Masonting Formation is composed of intertonguing volcanoclastic and hemipelagic sediments and overlies the Danao Limestone unconformably. It shows scattered distribution in Sogod Bay. The formation is dated Miocene to Pliocene (Florendo, 1984).

Inopacan Clastics is composed of well-sorted, rounded pebble to cobble conglomerate with poorly-bedded mudstone and calcareous tuff. It occurs in the northern, western and southern parts of the area. The Inopacan Clastics overlie unconformably the Pangasgan

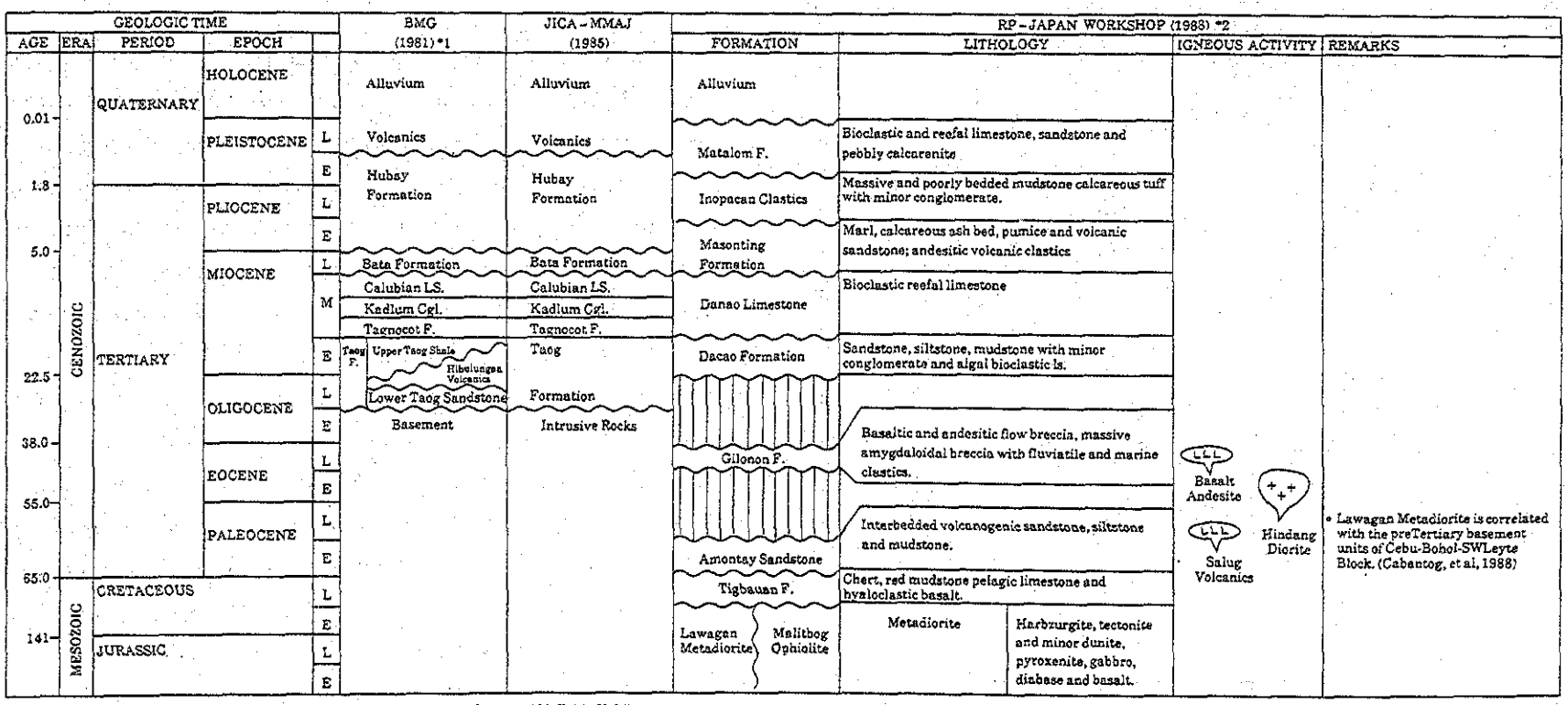

*1 BMG: Geology and Mineral Resources of the Philippines. 1981, Volume I P56 (Table II-24)
*2 A. Cabantog., et al., (ms. 1989)

Fig. -4 Stratigraphic Succession of SW Leyte

Formation correlated to the Masonting Formation and is dated Pliocene to Pleistocene (RP-Japan, 1985.).

Matalom Formation is a sequence consisting of calciclastics and shallow marine coralline limestone. The calciclastics are composed of calcarenite, calcisiltites and calucirudites with occasional calcareous mudstone. It occurs extensively almost over the whole area and overlies unconformably the Inopacan Clastics. The Matalom Formation is dated Pleistocene (RP-Japan, 1985).

2-2-1-2 NW Leyte (NLB) (Fig.-5)

The Northwestern Leyte Basin sequence represents deposits of the marginal basin. This basin is the northeastern segment of the Visayan Sea Basin. The structure of the area is dominated by NNW trending folds.

Taog Formation is the basement unit of the NLB. It is chiefly composed of conglomerate, sandstone, shale and thin interbeds of shaly limestone deposited during late Early Miocene. It occurs in the central part of the southern half of the area. The approximate thickness of the formation is about 2,100 m.

Tagnocot Formation is composed of massive and partly calcareous shale with thin interbeds of conglomerate, coarse sandstone and sandy shale. The unit is early Middle Miocene in age, unconformably overlying the Taog Formation. The approximate thickness of the unit is about 1,570 m.

Kadlum Conglomerate is composed essentially of matrix-supported conglomerate with occasional thin interbeds of shale and sandstone. The conglomerate is composed of well-rounded and poorly sorted pebble-sized clasts of andesite, quartz and chert set in sandy matrix. The formation is dated Middle Miocene (Corby, 1951). It occurs as small patches in the eastern coast at the northern end of the area. This formation is probably a deltaic deposit. The sequence has an observed thickness of 50 m and overlies unconformably the Tagnocot Formation.

Calubian Limestone is essentially a white coralline lenticular limestone with local marly and porous facies. It overlies conformably the Kadlum Conglomerate. It is equivalent to the Danao Limestone of SW Leyte deposited during the late Middle Miocene (Corby, 1951.).

Bata Formation is made up of shale and sandstone with local lenses of conglomerate and shaly limestone. The shale member is a massive unit composed of tuffaceous and locally bentonitic units. Sandstone is impregnated with bitumen. This formation has been considered a prospective source of rock asphalt deposits. It occurs extensively almost all over the area and overlies unconformably the Calubian Limestone. Approximate thickness of the sequence is about 900 m. The Bata Formation is dated Late Miocene (Pilac, 1965.)

Hubay Formation is composed of porous coralline limestone with minor occurrences of conglomerate, sandstone and shale as basal units. It occurs extensively along almost all of the coastal part of NW Leyte Peninsula and overlies the Bata Formation. It is equivalent to the Matalom Formation of SLR formed during Pleistocene (Pilac, 1965). Approximate thickness of this formation is about 100 m.

2-2-1-3 Central Highland (CH)

Pangasugan Formation consists of coarse conglomerate and pyroclastics with occasional lenses of sandstone and tuffaceous shale. It flanks and rims the Central Highland Volcanics. The formation is chiefly made up of coarse conglomerate along the flanks of the Central Highland Volcanics (CHV), and grades into matrix-supported unit away from CHV. It is distributed widely almost all over the Central Highland. The age of this formation is Late Miocene to Early Pliocene (Pilac, 1965.)

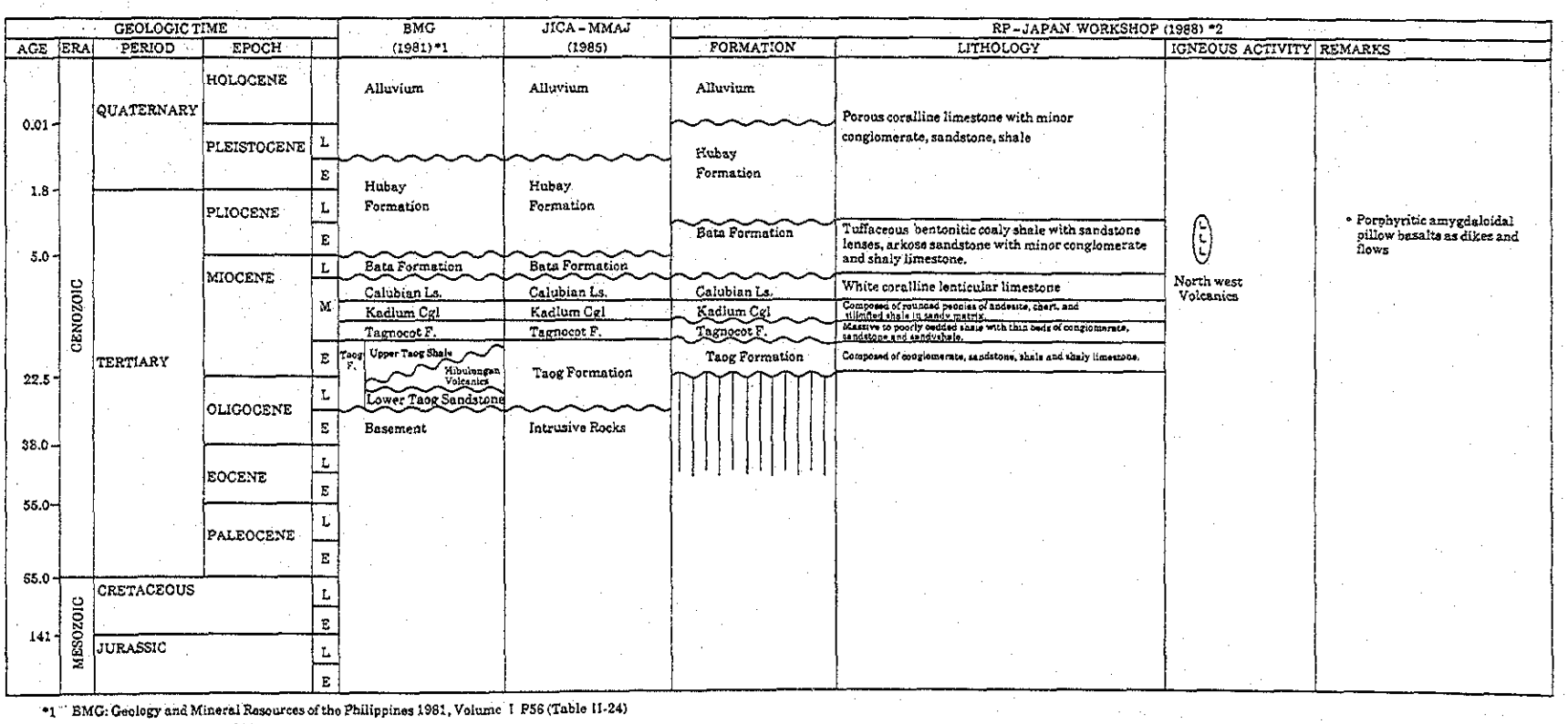

*1 BMG: Geology and Mineral Resources of the Philippines 1981, Volume I P56 (Table II-24)
*2 A. Cabantog., et al., (ms. 1989)

Fig. -5 Stratigraphic Succession of NW Leyte

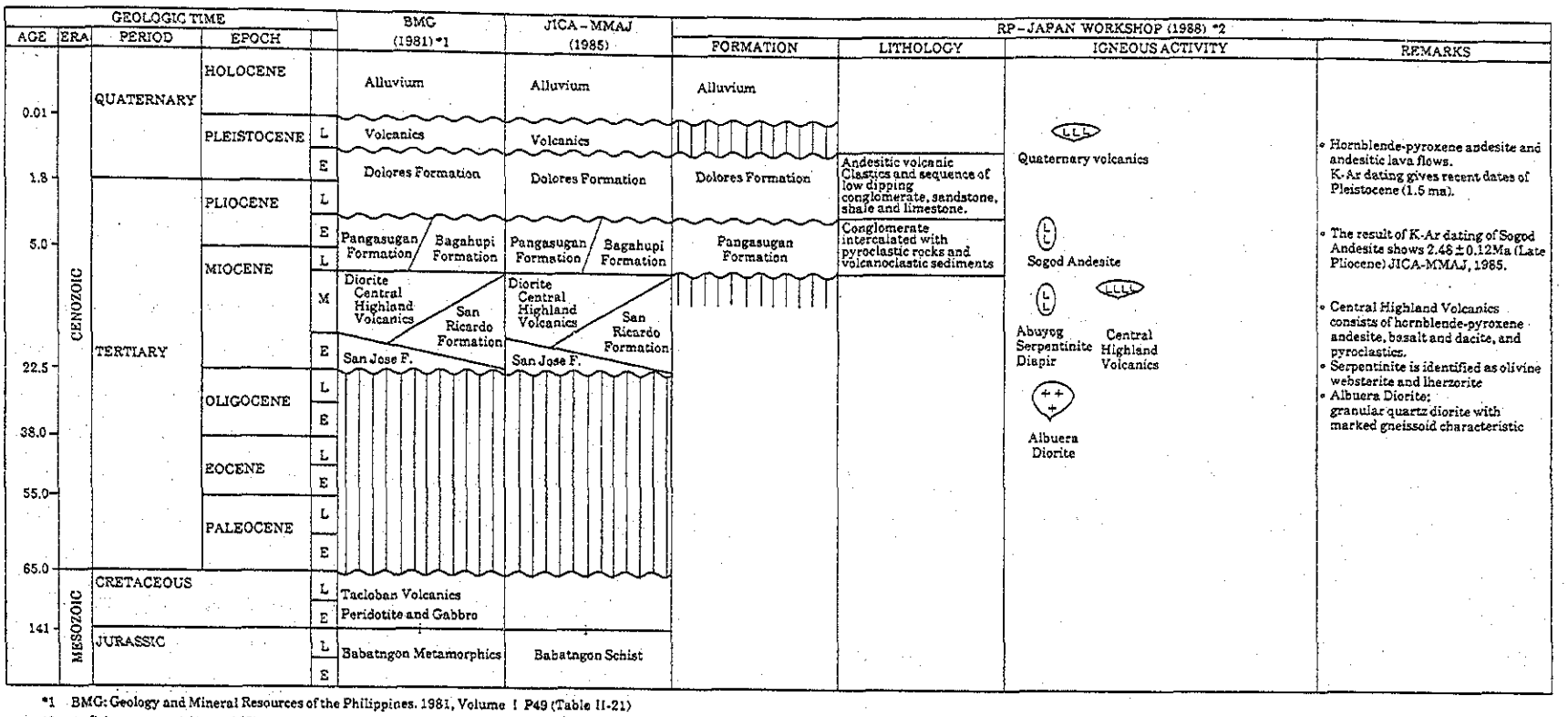

*1 BMG: Geology and Mineral Resources of the Philippines. 1981, Volume I P49 (Table II-21)

*2 A. Cabantog., et al., (ms. 1989)

Fig. -6 Stratigraphic Succession on Central Highland Leyte

Dolores Formation is composed of a matrix-supported volcano-sedimentary sequence occurring as flat-lying units mantling the slopes of the Central Highlands. This formation consists of andesitic volcanoclastics units, conglomerate, sandstone, shale and limestone. It overlies unconformably the Pangasugan Formation and is dated Late Pliocene to Pleistocene based on nanno plankton studies.

2-2-1-4 NE Leyte (NLR) (Fig.-7)

Babatngon Metamorphics is the oldest basement metamorphic rock unit in the area. It is pre-Cretaceous in age. The original rock unit is composed of intercallated sandstone, conglomerate, shale, cherty sediment and ferruginous shale. The schist was probably metamorphosed and deformed during the imbrication and emplacement of the Tacloban Ophiolite during the Paleogene. The metamorphic grade is green schist facies and is typically found in the Northern Tacloban Highlands at Babatngon and as small outcrops at Palo and Tanaun in the southern part of the area.

Tacloban Ophiolite consists of serpentinized harzburgite, undifferentiated gabbro, sheeted diabase dike complex, pillow basalt and pelagic sediments. The ophiolitic rocks characterized by northwesterly elongated patches are extensively distributed along the Tacloban Highlands from Babatngon to Tanaun, but they are mostly overlain by alluvial sediments in the southern part. It is believed that the Tacloban Ophiolite is similar to the Malitbog Ophiolite and was thrusted over the proto-rock units of the Babatngon Metamorphics leading to the metamorphism of these proto-rock units.

San Jose Formation is composed of slightly metamorphosed conglomerate, sandstone, shale and fine tuff units. It occurs as NW trending isolated hills found in the alluvial plains in the southern

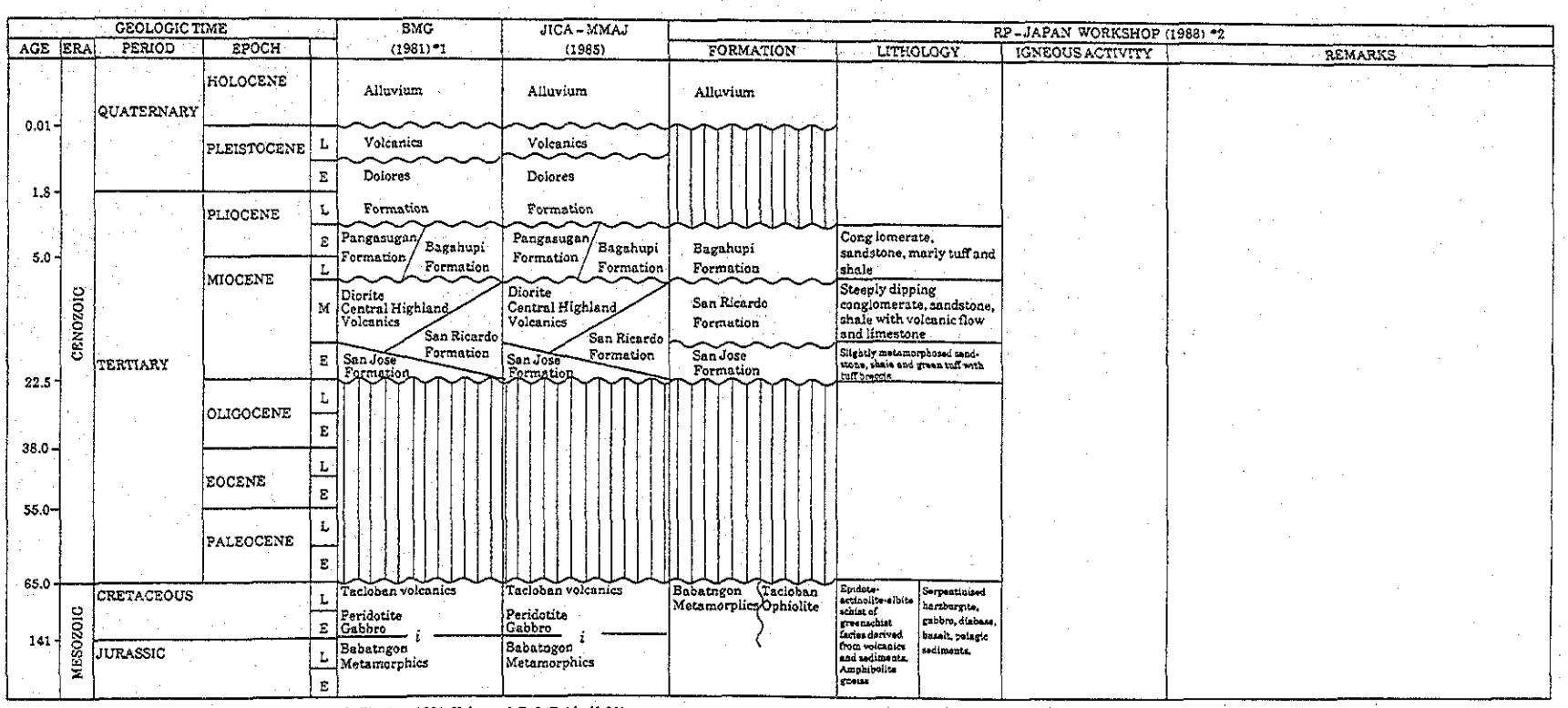

*1 BMG: Geology and Mineral Resources of the Philippines 1981, Volume I P49 (Table II-21)

*2 A. Cabantog., et al., (ms. 1989)

Fig. -7 Stratigraphic Succession of NE Leyte

part of the area. The age of this formation is Late Oligocene to Early Miocene. It has an estimated thickness of 950 m.

San Ricardo Formation consists of conglomerate, sandstone, shale with intercalated volcanic flows and thinly bedded to massive limestone. The beds are steeply dipping (60° to 70°) with occasional vertical dips and overturned beds. It occurs as patches along the NE slope of the Tacloban range and extends with a NW trend discontinuously from Tacloban City to Babatngon. The formation is observed overlying unconformably the Babatngon Schist and Tacloban Ophiolite. Its relationship with the San Jose Formation is also that of an unconformity. The age of the formation is Middle Miocene and apparent thickness of the sequence is about 650 m.

Bagahupi Formation is a sequence of sedimentary rocks made up of polymictic basal conglomerate, sandstone and marly tuffaceous shale. It occurs in the northeastern end of the area. The formation unconformably overlies the San Ricardo Formation and is dated Late Miocene to Pliocene. This formation is the youngest unit in the area.

2-2-2 Dinagat-Siargao Area

The stratigraphy of the Dinagat-Siargao Area is presented in accordance with the different physiographic subdivisions namely: Dinagat Island, Siargao-Bucas Grande Islands and Masapelid Island (Fig. 5, 8, 9 and 10). The survey conducted in this area is not yet adequate and so some problems remain to be resolved by later surveys.

2-2-2-1 Dinagat Island (Fig.-8)

Dinagat Ophiolite consists of the Ultramafic Complex (highly serpentinized peridotite and dunite), gabbro (Dongohan Gabbro) and diabase-basalt complex. The Ultramafic Complex occurs almost all over the island and is thrusted over the Gabbro and and the diabase-basalt complex. It has a K-Ar age of 84.8±4.2 m.a. corresponding to latest Middle Cretaceous (JICA-MMAJ, 1986.).

The Dongohan Gabbro is a small body of isotropic gabbro located in the eastern side of the Maliano-Loreto Valley. The diabase-basalt complex consists of diabase dike swarms and basalt flows. The diabase of the diabase-basalt complex is similar to the diabase dike which intruded the ultramafic rocks. Situated at a structurally higher position are the basalt flows which are commonly pillowed, amygdaloidal and have undergone some degree of spilitization. The diabase-basalt complex is distributed as small patches in the central part of the northern half of the island.

Nueva Estrella Amphibole Schist (NEAS) is disposed mainly on the southern part of Dinagat Island and is in thrust contact with the overlying Ultramafic Complex. The schistosity dips in the same direction as the thrust near the contact, but away from it, the attitude of the schistosity shows no preferred orientation. It is inferred that the protolith might be basic rocks and the age of the metamorphism is not much younger than the age of the ophiolite. The possibility that NEAS is older than the Dinagat Ophiolite is something that cannot be ignored (Sunga and Palaganas, ms., 1986). Near the thrust zone, the ultramafic rocks are highly serpentinized.

Loreto clastics consist of polymictic conglomerate, calcareous sandstone and shale. The conglomerate contains pebbles of basalt, diabase, serpentinized peridodite and schists. It occurs at the western side of Dinagat Island and overlies unconformably both the Dinagat Ophiolite and the Nueva Estrella Amphibole Schist. The age of the formation is Eocene. Malicdem (1963) stressed that a sequence of barren or undiagnostic sediments were observed overlying the definitely dated Eocene clastics and these sediments were deposited during the Oligocene.

Siargao Formation consists mainly of thickly bedded to massive limestone. The age of the formation is dated Miocene to Pleistocene based on paleontological data, but there is a possibility that the Siargao Formation is composed of two conformable limestone. Available data during the survey is not enough to separate these two beds (Sunga and Palaganas, 1986.). The Surigao Formation

GEOLOGIC TIME					BMG (1981)*1	JICA - MMAJ (1985)	RP - JAPAN WORKSHOP (1988) *2			
AGE	ERA	PERIOD	EPOCH				FORMATION	LITHOLOGY	IGNEOUS ACTIVITY	REMARKS
0.01	CENOZOIC	QUATERNARY	HOLOCENE		Alluvium	Alluvium	Alluvium			
			PLEISTOCENE	L	Siargao Formation (SF)	SF_2 (Siltstone, sandstone)	Siargao Formation	Oolitic, porous or dense limestne		
				E						
1.8		TERTIARY	PLIOCENE	L						
				E						
5.0			MIOCENE	L		SF_1 (Limestone)				
				M						
				E						
22.5			OLIGOCENE	L	Sapao Formation (SaFv)					
				E						
38.0			EOCENE	L		Pgl (Conglomerate, sandstone, chert)	Loreto clastics	Conglomerate with calcareous sandstone and shale		
				E						
55.0			PALEOCENE	L		SaFc2 (Tuffaceous sand-siltstone)				
				E		$SaFc_1$ (Basalt, andesite, diabase)				
65.0	MESOZOIC	CRETACEOUS PRE-CRETACEOUS			Ultramafic	Uc3 (Microgabbro, Pyroxenite) Uc2 (Dunite) Uc1 (Pyroxene peridotite)	Nueva Estrella Amphibole Schist	Amphibole schist with quartz vein		
							Dinagat Ophiolite — Diabase-Basalt Complex	Dike swarms of diabase and pillow basalt flows		
							Dongohan Gabbro	Gabbro		
						BC (Schistose gabbro)	Ultramafic Complex	Dunite, peridotite		

* The result of K-Ar dating of Ultramafic Complex shows 84.8±4.2Ma (latest Mid Cretaceous) JICA-MMAJ, 1986

*1 BMG: Geology Map (Scale 1:50,000) 4149 I ~ IV. 1983.
*2 Sunga and Palaganas., ms., 1986. " Geology and Mineral Resources of Dinagat Island Group ".

Fig. -8 Stratigraphic Succession of Dinagat Island

GEOLOGIC TIME AGE	ERA	PERIOD	EPOCH		BMG (1981) *1	JICA – MMAJ (1985)	RP – JAPAN WORKSHOP (1988) *2 FORMATION	LITHOLOGY	IGNEOUS ACTIVITY	REMARKS
0.01	CENOZOIC	QUATERNARY	HOLOCENE		Alluvium	Alluvium	Alluvium			
			PLEISTOCENE	L	Siargao Formation (SF)	SF_2 (Siltstone, sandstone)	Siargao Formation	Oolitic, porous or dense limestone interbedded carbonaceous shale		
1.8				E						
		TERTIARY	PLIOCENE	L						
5.0				E						
			MIOCENE	L						
				M		SF_1 (Limestone)				
22.5				E						
			OLIGOCENE	L	Sapao Formation (SaFv)					
				E						
38.0			EOCENE	L		Pg1 (Conglomerate, sandstone, chert)				
				E						
55.0			PALEOCENE	L		SaFc2 (Tuffaceous sand-siltstone)				
				E		$SaFc_1$ (Basalt, andesite, diabase)				
65.0	MESOZOIC	CRETACEOUS PRE-CRETACEOUS			Ultramafic	Uc3 (Microgabbro, Pyroxenite) Uc2 (Dunite) Uc1 (Pyroxene peridotite)	Dinagat Ophiolite: Sapao Formation	Diabase -basalt complex with tuff and tuffaceous sedimentary rocks		• Ultramafic Complex is correlated to Dinagat Ultramafic Complex;namely 84.8±4.2 ma, latest Mid Cretaceous (Sunga and Palaganas. ms., 1986).
						BC (Schistose gabbro)	Ophiolite: Ultramafic Complex	Dunite, peridotite		

*1 BMG: Geology Map (Scale 1:50,000) 4149 I ~IV. 1983.
*2 Sunga and Palaganas., ms., 1986. Geology and Mineral Resources of Dinagat Island Group.

Fig. -9 Stratigraphic Succession on Siargao and Bucas Grande Island

unconformably overlies the Loreto Clastics and occurs along the northwestern to western coast of Dinagat Island.

2-2-2-2 Siargao-Bucas Grande Islands

Dinagat Ophiolite consists of the Ultramafic Complex (serpentinized peridotite, dunite and pyroxenite) and the Sapao Formation which is composed of diabase dike swarms and pillow basalt. It is equivalent to the Dinagat Ophiolite in Dinagat Island. The Ultramafic Complex occurs extensively in the northern half of Bucas Grande Island. It is dated as Middle Cretaceous. The Sapao Formation is correlative to the diabase-basalt complex in Dinagat Island.

Occasionally, tuff and tuffaceous sandstone, siltstone and shale are found intercalated with the basalt flows. The rock unit was formed in the latest stage (Late Cretaceous) of the ophiolite detachment process. It occurs in the northern and central part of Siargao Island and in the northern part of Bucas Grande Island.

Siargao Formation consists of massive limestone with intercalated lenses of carbonaceous shale and sandstone and is correlated to the Siargao Formation in Dinagat Island, although the latter has no intercalated clastic member. The clastic rocks consist of materials derived from the ultramafic rocks which supports the idea of its unconformable relationship with the Ultramafic Complex. In the Siargao-Bucas Grande Area, the formation equivalent to the Loreto Formation in Dinagat Island is absent. It occurs nearly all over the Siargao Island and the southern part of the Bucas Grande Island and the age of the formation is Miocene to Pleistocene.

GEOLOGIC TIME AGE	ERA	PERIOD	EPOCH		BMG (1981) *1	JICA – MMAJ (1985)	RP – JAPAN WORKSHOP (1988) *2 FORMATION	LITHOLOGY	IGNEOUS ACTIVITY		REMARKS
0.01	CENOZOIC	QUATERNARY	HOLOCENE		Alluvium	Alluvium	Alluvium				
			PLEISTOCENE	L	Siargao Formation (SF)	SF_2 (Siltstone, sandstone)					
1.8				E							
		TERTIARY	PLIOCENE	L							
5.0				E							• Mabuhay Andesite is assumed to have erupted during the Late Miocene in Surigao del norte (Santos., et al., 1962)
			MIOCENE	L							
				M		SF_1 (Limestone)	Timamana Limestone	Limestone with shale, sandstone and chert.	Mabuhay Andesite		
				E			Masapelid Formation	Shale interbedded sandstone and conglomerate			
22.5							Bacuag Formation	Basalt flow with basaltic agglomerate	Basalt		
			OLIGOCENE	L	Sapao Formation (SaFv)						
				E							
38.0			EOCENE	L		Pg1 (Conglomerate, sandstone, chert)					
				E							
55.0			PALEOCENE	L		SaFc2 (Tuffaceous sand-siltstone)					
				E		$SaFc_1$ (Basalt, andesite, diabase)					
65.0	MESOZOIC	CRETACEOUS PRE-CRETACEOUS			Ultramafic (U)	Uc3 (Microgabbro, Pyroxenite) Uc2 (Dunite) Uc1 (Pyroxene peridotite)					
						BC (Schistose gabbro)					

*1 BMG: Geology Map (Scale 1:50,000) 4149 I ~IV. 1983.
*2 Sunga and Palaganas., ms., 1986. Geology and Mineral Resources of Dinagat Island Group.

Fig. -10 Stratigraphic Succession of Masapelid Island

2-2-2-3 Masapelid Island (Fig.-10)

Bacuag Formation consists of basaltic flows with intercalated basaltic agglomerate and clastic sediments of basaltic derivation. This rock sequence was intruded by fine basaltic dikes. This formation is the oldest unit in the island and is distributed in the northeastern part. The unit is believed to be of Late Oligocene to Early Miocene age.

Masapelid Formation is composed of interbeds of shale and calcareous sandstone with lenses of conglomerate, thin limestone beds and occasional coal seams. The shale member is fissile and breaks into thin slabs upon application of pressure. The clasts are mainly basaltic in composition (Abarquez, et al., 1980). The relationship to the underlying Bacuag Formation is conformable. The age of this unit is Early Miocene, possibly extending up to Middle Miocene (Sunga and Palaganas, 1986). It occurs as a small patch in the northern-central part of the island.

Timamana Limestone is composed of limestone which is white, massive, dense, fine - grained and slightly marbolized. It occurs in the northwestern part of the island and overlies the Masapelid Formation conformably. The tentative age of this unit is Middle Miocene (Sunga and Paraganas, 1986).

2-3 Geologic Structures

The geologic evolution and structures of the Leyte and Dinagat-Siargao Areas are intimately associated with the Philippine Trench and the Philippine Fault. The former is a NNW trending offshore structure of the area, along which the Philippine Plate is now subducting. The latter is inferred to be a left lateral strike slip fault and traverses the central part of the Leyte Island, parallel to the Philippine Trench. The movement along the Philippine Fault is continuous to the present time.

2-3-1 Leyte Area

In this area, the Tertiary to Quaternary sedimentary and volcanic units were formed by activities associated with the subduction along the Philippine Trench. Subsequent deformations were probably related to movements of the Philippine Fault. The complicated topography of Leyte Island reflect the complex interaction of the different geologic processes operative in this area.

The NNW-trending Philippine Fault traverses the central portion of Leyte Island. This major fault zone extends from Lingayen Gulf in the north to eastern Mindanao in the south and is traceable over 1,200 km. in length. The fault zone that defines the Philippine Fault in Leyte Island consists of several branches that cut across the Central Highland. The bifurcation of the fault lines caused graben development and occasional trapped valleys (e.g. Lake Danao). Block movements had brought about crustal uplifts and regional upwarp with associated basin development on the downthrown portions. A good example is the Calubian- Ormoc Basin. The splice apparently has its point of origin in Calubian that develops into multiple splices in the Ormoc area, roughly defining the fan-shaped Calubian-Ormoc Basin and Ormoc Bay. This

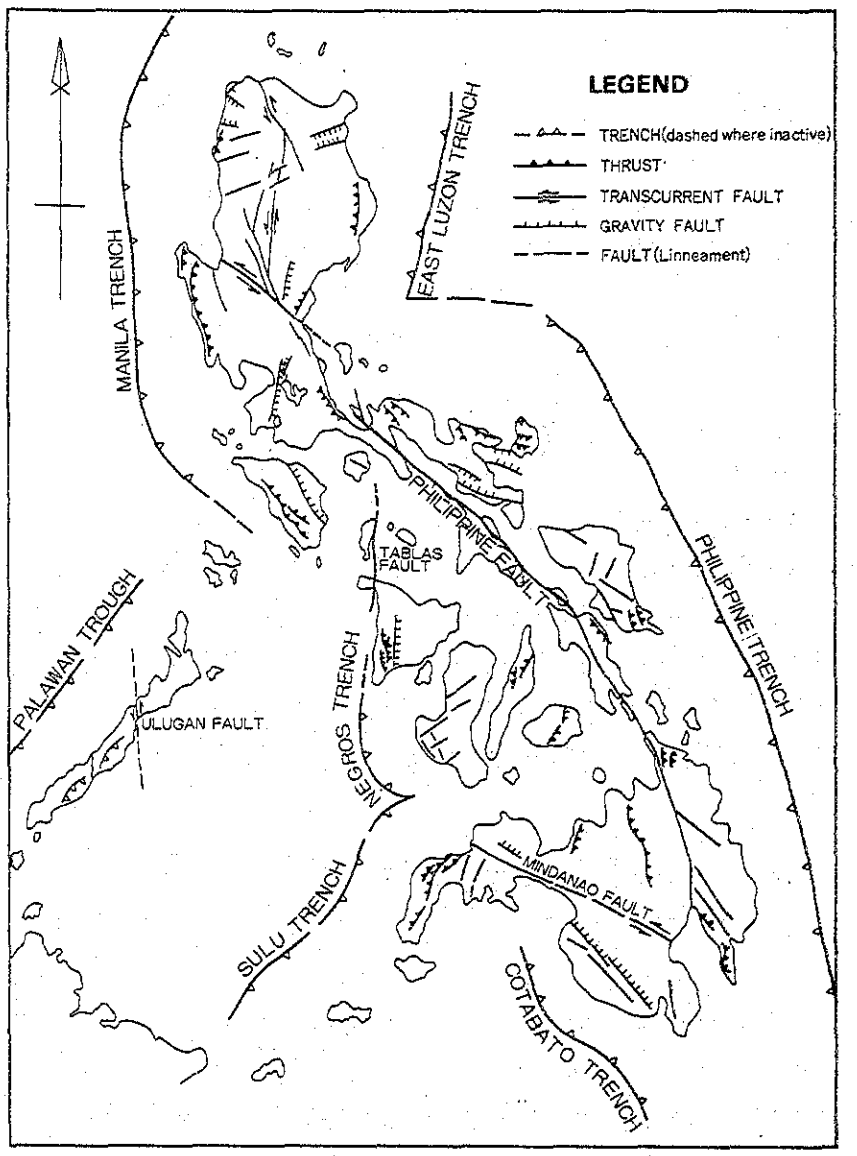

Fig. -11 Structural Map of Philippines

structural development could have led to the formation of a graben. Similar grabens encountered in many places of Leyte Island could have developed through the same geologic processes.

Gravity faults on these graben zones could have provided channelways for later hydrothermal fluids. Mineralization in this area is thus associated with these late stage tectonic activities. These fractures have played significant roles as the ascending channels of the auriferous epithermal ore solutions (e.g. Saint Bernard, Sogod)

In terms of fold structures, a N-S to NNW trending anticline extends from NW Leyte to SW Leyte. Folds on the NE Leyte area, which show the same features as that of the western anticline, form the Tacloban Range.

The Early Miocene Central Highland Volcanics crop out along the Philippine Fault zone area, often assuming the same trend of elongation, as the traces of fault movements. The Quaternary Volcanics are also distributed along the fault zone.

2-3-2 Dinagat-Siargao Area

The Dinagat Island Group, with the exception of Masapelid Island, is characterized by extensive exposures of ophiolitic basement rocks. This island group lies between two major tectonic features: the Philippine Fault and the Philippine Trench. Several sets of delineated major faults which generally trend NW are evidently reflected by the structural distribution of the different lithologic units underlying the islands. Transecting this NW faults

are numerous complementary NE trending faults. The faults are characterized by intense shearing, brecciation and thick gougy materials. A major thrust defines the tectonic contact between the Ultramafic Complex and the Nueva Estrella Amphibole Schist (NEAS). This thrust was caused by the overriding of the Dinagat Ophiolite upon the basement rocks. Trends of schistosities of NEAS observed near the thrust contact are almost parallel to the tectonic contact. In addition to this, exposed outcrops in Dinagat Island show a thrust contact between the diabase-basalt complex and the Ultramafic Complex. A thrust contact also defines the boundary the Dongohan Gabbro and the Ultramafic Complex.

In the Dinagat Island, NW to NNE trending folds are observed in the Ultramafic Complex, the Siargao Formation and the Loreto Clastics. These fold structures are believed to be the reflection of the older basement structures. Layerings and Foliations are the magmatic structures recognized in some parts of the ultramafic rocks reflecting magmatic differentiation. Layering is likewise exhibited by several chromite bodies interlayered with dunite particularly in the Talisay, Masdang and Mt. Redondo area.

2-4 Igneous Activities (Fig.-2, Fig.-12)

In this area, three major igneous activities are recognized as follows:

(1) Cretaceous igneous activities involving the formation of the ophiolite, followed by the emplacement of this upper mantle crust material over the pre-Cretaceous metamorphic basement rocks.

(2) Paleogene igneous activities which occurred in the Cebu-Bohol-Leyte block accompanied by subduction along the Tertiary East Philippine Arc (Mitchell, 1984).

(3) Post-Oligocene igneous activities associated with subduction along the Philippine Trench (Uyeda and Mac Cabe, 1982).

2-4-1 Leyte Area

Cretaceous igneous activities saw the formation of the Malitbog and Tacloban Ophiolites occurring in the southwestern and northeastern parts of the area respectively. The ophiolite complexes override the pre-Cretaceous metamorphic basement rocks.

The igneous activities along the East Philippine Arc formed the Salug Volcanics and brought about the intrusion of the Eocene Hindang Diorite. The post-Oligocene igneous activities associated with the subduction at the Philippine Trench formed Oligocene Albuera Diorite, Early Miocene Central Highland Volcanics, Early Pliocene Sogod andesite and Early Pleistocene Quaternary volcanics. The Early Miocene Central Highland Volcanics is made up of andesitic-basaltic flows, breccias and pyroclastic rocks while the Early Pliocene Sogod Andesite consist of andesitic flows. All of these rocks occur mainly in the Central Highland and Biliran Is.

These igneous activities are believed to be closely related to the Philippine Fault and occur along the fault zone. An upper mantle gliver called Abuyog Serpentine is intruded along the fault zone.

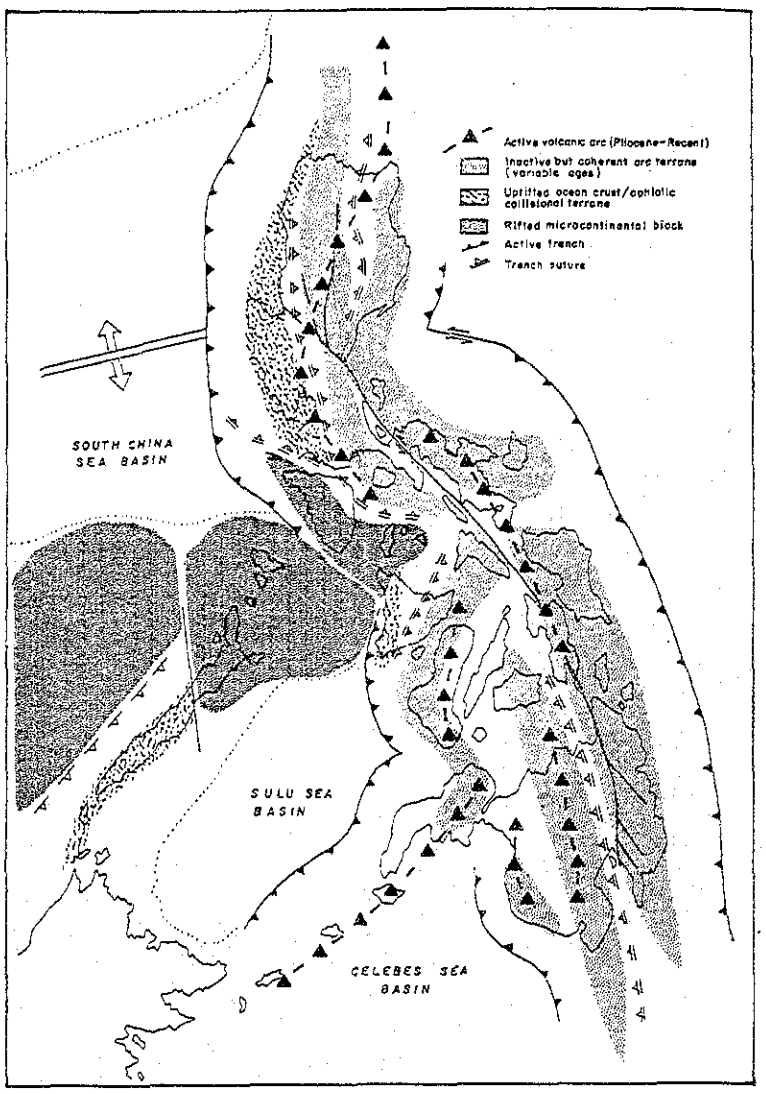

Fig.-12 Tectonic Terranes

Miocene to Pliocene volcanics occurs as small patches exposed along the anticline axis.

2-4-2 Dinagat-Siargao Area

The Cretaceous igneous activity resulted in the formation of the Dinagat Ophiolite presently exposed in Dinagat, Siargao and Bucas Grande Islands.

Products of Tertiary and Quaternary igneous activities are not observed in the above mentioned islands.

In Masapelid Is., Oligocene igneous activities led to the formation of the basalt flows of the Bacuag formation as observed in the northeastern part. The Late Miocene Mabuhay Andesite, the origin of which is intimately related to the subduction event along the Philippine Trench, covers the central part of the island.

2-5 Mineralization and Major Mineral Showings

Three types of mineralization in Leyte and two types in Dinagat-Siargao are recognized.

The list of surveyed mineral showings is shown in Table-1 and 2. (The numbers in the bracket correspond to numbers in the Attached P1-7)

Leyte Area

The three types of mineralization recognized in Leyte are as follows:

Table 1 Surveyed Mineral Showings in Leyte Area

*1 MINERAL SHOWING NAME	LOCATION	COMMODITY AND MINERALIZATION	AGE	TECTONIC PROVINCE	DESCRIPTION	
					OCCURRENCE	CHEMICAL ASSAY OF SAMPLE
16 Mt Bagacay (Lambonao)	124°58' E 10°07' N	Cu Vein	Neogene	Volcanic-plutonic arc	Hydrothermal vein and dissemination in andesite, basalt and pyroclastics	Channel sample of altered zone Au tr, Ag 1 g/t, Cu 0.01%, Pb 0.01%, Zn 0.03%
17 Maasin	124°51' E 10°11' N	Ni Residual	Post Cretaceous	Oceanic crust	Nickeliferous laterite	Laterite sample Au tr, Ag 1 g/t, Cu 0.01%, Pb 0.23%, Zn 0.01%
22 Ingan	125°10' E 10°27' N	Au Vein	Neogene	Volcanic-plutonic arc	Hydrothermal vein and dissemination in altered zone of andesite	Altered zone sample Au 0.1 g/t, Ag 1 g/t, Cu <0.01%, Pb 0.01%, Zn 0.01%
23 Sogod	124°58' E 10°25' N	Cu Vein	Neogene	Volcanic-plutonic arc	Hydrothermal vein in altered zone of andesite	Altered zone sample Au 0.1 g/t, Ag 2 g/t, Cu 0.01%, Pb 0.06%, Zn 0.02%
25 Bagacay	124°56' E 11°17' N	Cu Stratabound massive sulphide	Late Cretaceous	Oceanic crust	Stratabound massive sulphide in basaltic lava flow	
26 Liberty	124°44' E 11°19' N	Peat	Quaternary	Fore arc basin	Deposited in quaternary sediments Value less	
30 Pansagan (Punpuan)	124°50' E 10°36' N	Mn Residual/ Mechanical	Post Cretaceous	Oceanic crust	Mined out (Manganese Wad)	Ore assay Mn 57.28%, Fe 0.08%, P 0.07%, S 0.07%, SiO_2 0.88%
31 Balite (Villalaba)	124°25' E 11°12' N	Asphalt	Neogne	Back arc basin	Occurs in Mio. - Pliocene sediments	
33 Biliran	124°31' E 11°19' N	Native sulphur	Recent	Plutonic-volcanic arc	Occurs around volcano	
40 Pulta	124°51' E 10°26' N	Au, Cu Vein	Neogene	Volcanic-plutonic arc	Hydrothermal vein in diorite with strong alteration	
41 Curajo	124°58' E 11°11' N	Cu Stratabound massive sulphide	Late Cretaceous	Ocean crust	Stratabound massive sulphide in basaltic lava flows and metasediments	Average values of 6 drillings Au 0.75 g/t, Ag 3.67 g/t, Cu 0.41%, Pb tr, Zn 0.21%
46 Antipolo	124°46' E 11°06' N	Ni Vein	Neogene	Volcanic-plutonic arc	Hydrothermal vein in serpentinized peridotite	Ore assay (K100706) 0.65% Ni (Average values of vein Ni 0.2~0.7%)
48 Caibaan	124°59' E 11°12' N	Cu Stratabound massive sulphide	Late Cretaceous	Ocean Crust	Stratabound massive sulphide in basaltic lava flows and metasediments	Ore assay (K100903) Au 0.02 g/t, Ag 25.78 g/t, Cu 1.64%, Pb tr, Zn 0.21%
49 Ormoc	124°59' E 11°01' N	Bentonite Clay	Neogene	Back arc basin	Shale altered by hydrothermal solution	
50 Suhi	124°56' E 11°19' N	Cu Vein	Neogene	Volcanic-plutonic arc	Hydrothermal vein in crystalline-schist	Ore assay (AVC-04-101085) Au 0.015 g/t, Ag 9.3 g/t, Cu 10.4%, Pb tr, Zn 0.39%
51 Pinut-an	125°17' E 10°09' N	Au Vein	Neogene	Volcanic-plutonic arc	Gold-bearing quartz vein in plagiophyric andesite	Altered zone sample Au g/t / Ag g/t / Cu % / Pb % / Zn % (1) tr / 5 / 0.07 / 0.06 / 0.01 (2) 0.4 / 2 / tr / 0.03 / 0.02
52 Anilao	125°09' E 10°08' N	Cu Vein	Neogene	Volcanic-plutonic arc	Epithermal veinlets and disseminations in altered basic rocks (mainly serpentinized peridotite)	Altered zone sample Au 1.8 g/t, Ag 29 g/t, Cu 4.88%, Pb 0.02%, Zn 0.02%,

*1 These numbers correspond to the numbers in Attached Plate-8.

(A) Massive sulphide type mineralization

This type occurs in pillow basalts and pelagic sediments of the Tacloban and Malitbog Ophiolites and is mainly composed of pyrite and chalcopyrite (Example: 25. Bagacay, 41. Curajo, 48. Caibaan).

(B) Vein Type Mineralization

This type mainly occurs as copper rich fissure-filling mineralization in the Central Highland Volcanics (16. Mt. Bagacay, 22. Ingan, 23. Sogod, 40. Pulta, 46. Antipolo, 50. Suhi, 51. Pinut-an, 52. Anilao). They are associated with the gold-bearing ascending solutions and are usually noted along grabens formed by gravity faulting (Example: Saint Burnard, Sogod). In one special case, a nickeliferous vein formed from extracted solution of Ni from the host ultramafic rocks is observed (Example: Antipolo)

(C) Residual Type concentration

This type is observed as nickeliferous laterite formed through the alteration of the ultramafic rocks of the Cretaceous Malitbog Ophiolite. Manganese wads altered from manganese nodules of the Miocene to Pliocene Pangasgan Formation are also present (Example: 17. Maasin, 30. Pansagan)

Pinut-an Mine

This mine has been operated intermittently in the past.

It is located in the southern part of the northeast coast of Panaon Is., in Southwestern Leyte. Host rock is argillized and silicified plagioclase porphyry andesite. Ore minerals include native gold, pyrite and sphalerite in quartz veins. The intermittent operation was carried out by Benguet Exploration Inc. Production rate was 5 MTD, Crude ore grade: Au 10 - 17

Table 2 Surveyed Mineral Showings in Dinagat-Siargao Area

MINERAL *1 SHOWING NAME	LOCATION	COMMODITY AND MINERALIZATION	AGE	TECTONIC PROVINCE	DESCRIPTION	
					OCCURRENCE	CHEMICAL ASSAY OF SAMPLE
① Talisay	125°39' E 10°27' N	Cr Orthomagmatic	Cretaceous	Oceanic crust	Massive and disseminated chromite band in dunite (Mined out)	Chromite condensed sample Cr_2O_3 41.01%, Al_2O_3 8.83%, FeO 11.29%, MgO 20.20%, SiO_2 12.00%
② Masdang	125°39' E 10°26' N	ditto	ditto	ditto	ditto	Chromite condensed sample Cr_2O_3 36.78%, Al_2O_3 8.72%, FeO 10.97%, MgO 22.33%, SiO_2 17.49%
⑤ Velore	125°34' E 10°09' N	ditto	ditto	ditto	Massive and dissseminated chromite band in dunite (produced about 10,000MT of chromite. Mined out)	Chromite condensed sample Cr_2O_3 29.82%, Al_2O_3 13.05%, FeO 11.33%, MgO 23.11%, SiO_2 18.38%
⑬ Redondo	125°38' E 10°22' N	ditto	ditto	ditto	Massive and disseminated chromite band in dunite. (Mined out)	Chromite condensed sample Cr_2O_3 47.56%, Al_2O_3 11.49%, FeO 13.25%, MgO 19.62%, SiO_2 7.96%
⑭ Tagbaboy (1)	125°28' E 10°03' N	ditto	ditto	ditto	ditto	Chromite condensed sample Cr_2O_3 35.64%, Al_2O_3 11.90%, FeO 12.83%, MgO 21.68%, SiO_2 14.29%
Tagbaboy (2)	125°37' E 10°02' N	ditto	ditto	ditto	ditto	Chromite condensed sample Cr_2O_3 50.05%, Al_2O_3 9.74%, FeO 16.29%, MgO 15.37%, SiO_2 8.07%
⑮ Cangumod	125°39' E 9°41' N	Au Hydrothermal Vein	Neogene	Volcanic-plutonic arc	Gold-bearing quartz vein (Mined out)	Vein samples (Outcrops) Au g/t / Ag g/t / Cu % / Pb % / Zn % (1) <0.01 / 1 / 0.02 / 0.01 / 0.02 (2) 10.8 / 6 / 0.02 / 0.01 / <0.01
⑯ Avelina	125°33' E 10°05' N	Cr Orthomagmatic	Cretaceous	Oceanic crust	Massive and disseminated chromite band in dunite	Chromite condensed sample Cr_2O_3 46.99%, Al_2O_3 11.84%, FeO 13.46%, MgO 17.81%, SiO_2 6.65%

*1 These numbers correspond to the numbers in Attached Plate-8.

g/MT, ore reserves estimated at 79,910 MT, average grade Au : 9.75 g/MT and Ag : 12.81 g/MT.

Dinagat-Siargao Area

(A) Orthomagmatic type mineralization

The orthomagmatic chromite mineralization is believed to have occurred through magmatic differentiation processes that characterized the formation of the Dinagat Ophiolite. The chromite-rich zones are usually associated with dunites. The northern part of Dinagat Is. is characterized by layered chromites whereas the central to southern parts host podiform type chromites (Example: (1) Talisay, (2) Masdang, ⑬ Redondo, ⑭ Tagbaboy, (⑯ Avelina)

(B) Vein type mineralization

This type is observed in the argillized Miocene Mabuhay Andesite as gold bearing quartz veins (Example: ⑮ Cangumod).

In addition to the above mentioned mineralization, nickeliferous laterite type of concentration similar to that of Nonoc Mine is suspected to be present in the southern part of Dinagat Island. However, the present work in that particular area did not reveal such mineral showing.

3. Geochemical Sample Analyses and Data Processing

3-1 Analytical Methods and Precision

3-1-1 Analytical Methods

The survey area was divided into unit cells measuring 2 km (N-S) by 2 km (E-W). The datum point is at long 121°45'E, lat 9°00'N. Chemical data of the stream sediment samples (JICA-MMAJ., 1986-1988) were statistically analyzed through the following four methods.

All data presented here are divided into three populations, Samar, Leyte and Dinagat-Siargao.

(1) Univariate analyses of the geometrical average values (hereinafter called cell average values) of the geochemical analyses data in each cell.
(2) Univariate analyses of the moving average values, where a frame consisting of nine cells (three cells in both N-S and E-W directions) is set and the average value of the nine cells is taken to be the value of the central cell. The frame is moved one cell at a time throughout the survey area and the average for every step is calculated.
(3) Univariate analyses of the high-pass filter values -- the positive differences between the cell average and the corresponding moving average values.
(4) Multivariate analyses (Factor analyses) of the cell average values.

The following are the number of samples, cells and chemical analyses components which were prepared for the above analyses.

Table-3 Details of Samples and Cells

Area	Number of Samples	Number of Cells	Components for Analysis
Samar	1,309	542	Cu, Pb, Zn, Ag, As, Mn, Ni, Co, Hg, Cr
Leyte	5,064	1,734	Cu, Pb, Zn, Ag, As, Mn, Ni, Co, Mo, Hg
Dinagat-Siargao	766	292	Cu, Pb, Zn, Ag, As, Mn, Ni, Co, Hg, Cr

An IBM 3084Q computer and statistical analyses package BMD 08M 1(UCLA developed) were utilized for statistical procedures. Computation was done in logarithmic values then subsequently converted into normal values. For the purpose of statistical procedure, the 50 percent value of the detection limit value was taken as the value of sample below the detection limit.

Chemical analyses of Samar and Northern Leyte samples were conducted in PETROLAB, the chemical analysis section of the MGB, and those of Southern Leyte and Dinagat-Siargao were analyzed in CHEMEX CANADA (commercial laboratory) by using AAS. Detection limits of AAS are shown in Table-4.

Table-4 Detection Limits of AAS Analyses (ppm)

Element	Cu	Pb	Zn	Ag	As	Mn	Ni	Co	Mo	Hg	Cr
PETROLAB	2	10	2	1	0.5	50	3	3	2	0.04	100
CHEMEX Co.	2	1	1	0.1	0.5	5	1	1	1	0.005	50

3-1-2 Precision Check

Precision checks for the chemical analyses were carried out. The variance of the analyzed value at 95 percent confidence level was calculated by the Thompson and Howarth method (1973) with the result of the batch test.

A sample was chosen from each analysed batch (about 20 samples) and was analysed with another batch after which the variance was calculated statistically. The number of batch test samples for the entire RP-Japan Project is approximately 1,000 for Cu, Pb, Zn, As, Mn and Hg and approximately 800 for Ni and Co.

Table-5 Dispersion of Batch Test Results

Component	Dispersion	Component	Dispersion
Cu	±15%	Mn	±10%
Pb	±20%	Ni	±20%
Zn	±20%	Co	±20%
As	±25%	Hg	±25%

The variance for Ag, Mo and Cr values could not be determined because the results of many samples were below the detection limit.

3-2 Cell Average Values

As mentioned above, geometrical average values of the geochemical data in each cell were used in the analyses. For cells without any sampling point (blank cell), the following gap-filling process was carried out.

(1) Geometrical average of the eight cells around the blank cell is applied as the value of the blank cell (when the number of effective values was less than four, this process was not carried out).
(2) This gap-filling process was done twice.

3-2-1 Univariate Analyses of Cell Average Data of Samar

3-2-1-1 Basic statistical values

Basic statistical values of the cell average for each element in Samar are shown in Table-6. Basic statistical values of the original analytical results are also shown in Table-7 for reference. Regarding Pb, Ag and Hg over 95% cells show valus below detection

Table-6 Basic Statistical Values for the Cell Average Data

	Cu (ppm)	Zn (ppm)	As (ppm)	Mn (ppm)	Ni (ppm)	Co (ppm)	Cr (ppm)
M	37.59	75.37	1.77	715.66	77.44	26.34	1,675.86
M+1.0 σ	68.78	117.68	4.98	1,183.51	207.80	45.36	9,095.99
M+1.5 Mσ	93.04	147.02	8.37	1,521.96	340.39	59.54	21,191.22
M+2.0 Mσ	125.86	183.69	14.07	1,957.20	557.58	78.14	49,396.37
Maximum	139.00	280.00	31.00	2,728.50	1,544.00	94.98	90,188.00
Minimum	1.00	8.78	0.25	41.52	1.50	1.50	50.00
R.B.D.L	0.2%	0%	14.0%	0.2%	0.2%	0.9%	6.0%

R.B.D.L.: Ratio of cells below detection limit

Table-7 Basic Statistical Values of the Original Data

	Cu (ppm)	Zn (ppm)	As (ppm)	Mn (ppm)	Ni (ppm)	Co (ppm)	Cr (ppm)
M	40.46	75.76	1.47	742.80	79.56	27.01	1,554.16
M+1.0 σ	76.71	122.49	4.87	1,298.34	271.10	52.30	10,698.33
M+1.5 σ	105.70	155.75	8.87	1,716.51	500.44	72.76	28,068.91
M+2.0 σ	145.58	198.04	16.15	2,269.36	923.77	101.23	73,643.60
Maximum	740.00	894.00	95.00	3,840.00	2,700.00	270.00	150,000.00
Minimum	1.00	7.0%	0.25	25.00	1.50	1.50	50.00

limit, therefore Pb, Ag and Hg are omitted in the statistical analysis.

3-2-1-2 Histograms and cumulative frequency curves

Histograms and cumulative frequency curves showing the frequency distribution of the cell average values for each element were drawn (Attached P1. 1-10). Inflection point of the curve was selected by the Lepeltier's method (1969) and its corresponding cell average value was regarded as the lowest anomalous value (threshold value).

Inflection points for Pb, Ag and Hg could not be determined, because over 95 percent of the cell contained Pb, Ag and Hg values below the detection limits. Details of the inflection point for each element are shown in Table-8.

Table-8 Details of Inflection Points of the Cumulative Frequency Curves for Elements and Cell Average Values

Element	Cu	Zn	As	Mn	Ni	Co	Cr
Cumulative frequency	77%	83%	80%	80%	85%	82%	91%
Cell Average	60 ppm	110 ppm	4 ppm	100 ppm	170 ppm	40 ppm	13,000ppm

3-2-1-3 Correlation Coefficients of Analysed Elements

Correlation coefficients among elements of cell averages are shown in Table-9. Correlation coefficients among elements of the original analytical results are also shown in Table-10.

Table-9 Correlation Coefficients of the Cell Average Data

	Cu	Zn	Pb	Ag	As	Mn	Ni	Co	Hg	Cr
Cu	1.000									
Pb	-0.026	1.000								
Zn	0.455	0.090	1.000							
Ag	0.010	0.048	0.045	1.000						
As	-0.346	0.047	-0.115	0.061	1.000					
Mn	0.592	-0.027	0.737	-0.074	-0.298	1.000				
Ni	-0.231	-0.191	-0.285	-0.104	0.039	-0.091	1.000			
Co	0.417	-0.215	0.332	-0.148	-0.273	0.604	0.577	1.000		
Hg	0.111	0.134	-0.001	0.199	0.239	0.027	-0.081	-0.013	1.000	
Cr	-0.446	0.108	-0.095	-0.069	0.144	-0.126	0.791	0.406	-0.127	1.000

Table-10 Correlation Coefficients of the Original Analyses Results

	Cu	Pb	Zn	Ag	As	Mn	Ni	Co	Hg	Cr
Cu	1.000									
Pb	-0.027	1.000								
Zn	0.448	0.123	1.000							
Ag	0.019	0.472	0.114	1.000						
As	-0.235	0.095	-0.058	0.097	1.000					
Mn	0.529	-0.079	0.589	-0.090	-0.256	1.000				
Ni	-0.127	-0.127	-0.286	-0.090	-0.022	-0.006	1.000			
Co	0.358	-0.195	-0.167	-0.122	-0.247	0.513	0.680	1.000		
Hg	0.072	0.255	0.055	0.302	0.240	-0.017	-0.083	-0.043	1.000	
Cr	-0.350	-0.051	-0.155	-0.050	0.047	-0.100	0.787	0.472	-0.093	1.000

Of the cell average values, positive correlation coefficient of more than 0.5 is observed among the following elements:

Cu-Mn, Zn-Mn, Mn-Co, Ni-Co, Ni-Cr

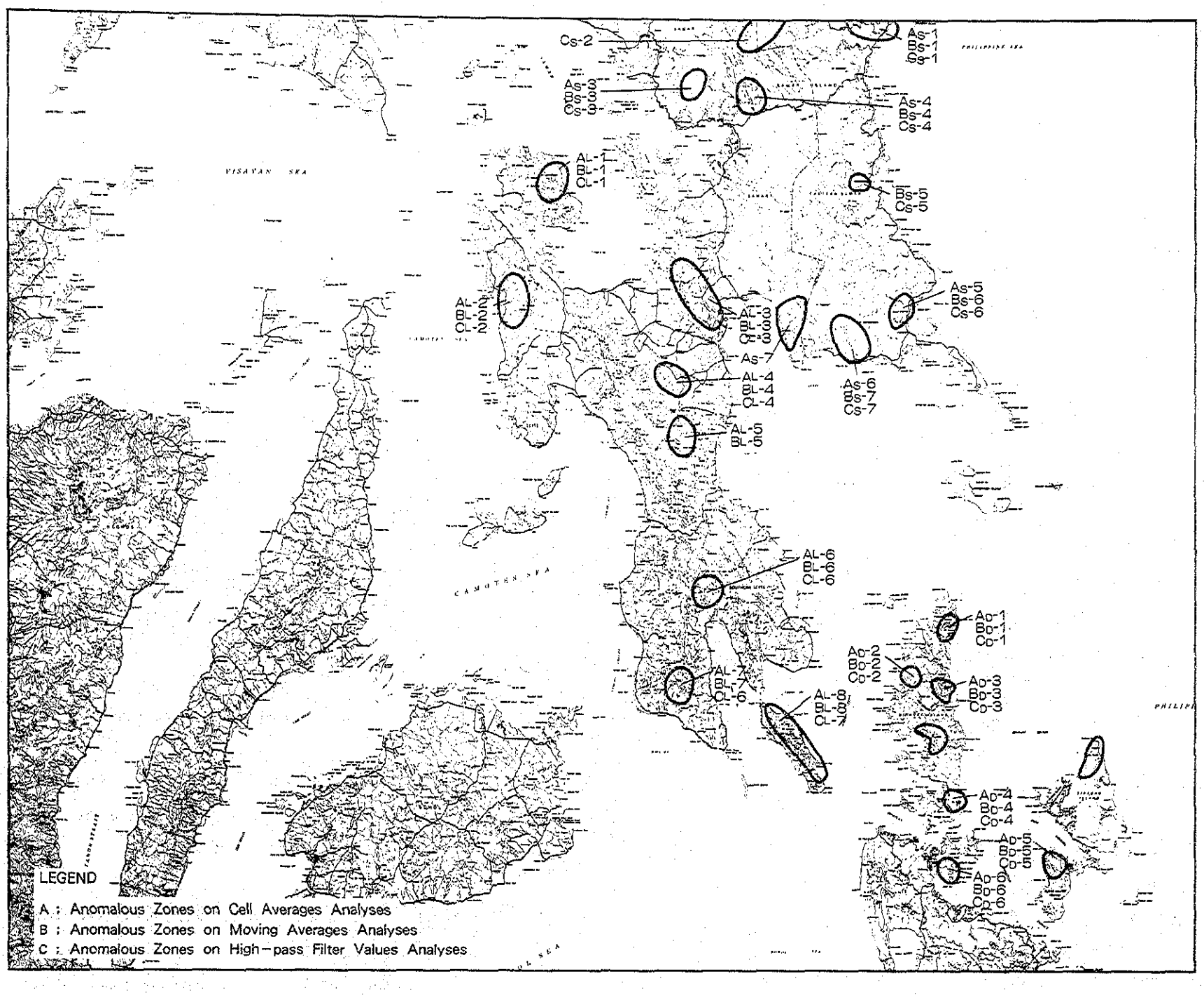

Fig. -13 Anomalous zones in Leyte and Dinagat-Siargao Area

3-2-1-4 Areal Distribution of the cell average values (Attached P. 2-1 No. 1 - No. 10)

The cell average values of each element were classified into eleven ranks and were plotted on a 1:1,000,000 scale map with corresponding rank color. The classified ranks are as follows.

Rank	Cumulative Frequency	Rank	Cumulative Frequency
A	$99\% \leqq Z$	G	$40\% \leqq Z < 50\%$
B	$95\% \leqq Z < 99\%$	H	$30\% \leqq Z < 40\%$
C	$90\% \leqq Z < 95\%$	I	$20\% \leqq Z < 30\%$
D	$75\% \leqq Z < 90\%$	I	Detection Limit $\leqq Z < 20\%$
E	$60\% \leqq Z < 75\%$		
F	$50\% \leqq Z < 60\%$	K	Detection Limit $> Z$

The area distribution of the anomalous cell averages are as follows (anomalous elements are shown in brackets). These localities are shown in Figure 13.

As-1: West side of Dolores in the east coast (Ni, Hg, Cr).

As-2: Central part of Samar (40 km west of Dolores) (Cu, Zn, Mn, Co).

As-3: Central-western part of Samar (12 km NNE of Catbalogan in the west coast) (As, Hg)

As-4: Central Part of Samar (13 km NNE of Wright in the west coast) (As, Mn, Hg)

As-5: Southeastern part of Samar (At the west side of General MacArthur) (Zn, As, Ni)

As-6: Southern part of Samar (At the north side of Balangiga in the south coast) (Ni, Co, Hg, Cr).

As-7: Southwestern part of Samar (20 km ESE of Basay in the south coast) (Cu, Zn, Mn, Ni, Co).

The significance of the relationships between these anomalous zones and mineralization are not yet fully understood because the geological survey of Samar is not yet completely finished.

Table-11 Basic Statistical Values of the Cell Average Data of Leyte

	Cu (ppm)	Zn (ppm)	As (ppm)	Mn (ppm)	Ni (ppm)	Co (ppm)	Hg (ppb)
M	44.13	111.46	2.10	978.01	31.82	28.06	28.33
M+1.0 σ	63.18	186.09	4.61	1,469.14	67.51	42.01	47.98
M+1.5 σ	75.60	240.45	6.82	1,800.62	98.34	51.41	62.43
M+2.0 σ	90.46	310.69	10.09	2,206.90	143.23	62.91	81.25
Maximum	4,100.00	442.40	77.46	4,500.00	1,487.20	89.24	4,899.00
Minimum	3.00	7.71	1.00	131.38	1.50	2.08	20.00
R.B.D.L.	0%	0%	0%	0%	0.2%	0%	80%

R.B.D.L. : Ratio of cells below detection limit.

Table-12 Basic Statistical Values of the Original Analytical Results of Leyte

	Cu (ppm)	Zn (ppm)	As (ppm)	Mn (ppm)	Ni (ppm)	Co (ppm)	Hg (ppb)
M	44.29	109.97	2.10	968.43	32.42	28.00	28.07
M+1.0 σ	66.96	201.26	5.18	1,615.24	73.62	45.38	53.87
M+1.5 σ	80.95	272.31	8.13	2,086.03	110.94	57.77	74.36
M+2.0 σ	101.22	368.44	12.77	2,694.05	167.17	73.55	102.64
Maximum	6,600.00	3,000.00	590.00	6,900.00	2,530.00	185.00	7,300.00
Minimum	1.00	3.00	0.60	25.00	1.50	1.50	20.00

3-2-2 Univariate Analyses of Cell Average Data of Leyte

3-2-2-1 Basic statistical values

Basic statistical values of the cell average value for each element are shown in Table-11. Basic statistical values of the original analytical results are also shown in Table-12 for reference.

In the chemical analysis results of Pb, Ag and Mo, over 95% cells show the values below the detection limits, so those elements are omitted from statistical procedure.

3-2-2-2 Histograms and cumulative frequency curves

Histograms and cumulative frequency curves showing the frequency distribution of the cell average values for each element were drawn (Attached P1. 1-10). Inflection point of the curve was selected by the Lepeltier's method (1969) and its corresponding cell average value was regarded as the lowest anomalous value (threshold value). Inflection points for Pb, Ag and Mo could not be determined because over 95 percent of the cell contained Pb, Ag and Mo values below the detection limits. Details of the inflection point for each element are shown in Table-13.

Table-13 Details of Inflection Point of the Cumulative Frequency Curves for Elements and Cell Average Values

Element	Cu	Zn	As	Mn	Ni	Co	Hg
Cumulative Frequency	95%	80%	85%	93%	83%	79%	94%
Cell Averages	69ppm	170ppm	5.5ppm	1,600ppm	57ppm	38ppm	70ppb

3-2-2-3 Correlation coefficients of analysed elements

Correlation coefficients among elements of cell averages are shown in Table-14. Correlation coefficients among elements of the original analytical results are also shown in Table-15.

Table-14 Correlation Coefficients of the Cell Average Data

	Cu	Pb	Zn	Ag	As	Mn	Ni	Co	Mo	Hg
Cu	1.000									
Pb	0.346	1.000						N:1,734		
Zn	0.213	0.083	1.000							
Ag	0.329	0.654	0.052	1.000						
As	0.057	0.237	-0.319	0.136	1.000					
Mn	0.217	0.073	0.615	-0.068	0.005	1.000				
Ni	0.030	0.111	-0.340	0.091	0.305	0.052	1.000			
Co	0.265	0.029	0.660	0.014	-0.390	0.646	0.134	1.000		
Mo	0.057	0.098	-0.152	0.021	0.458	0.169	0.199	-0.134	1.000	
Hg	0.205	0.376	0.017	0.417	0.255	0.001	-0.089	-0.091	0.018	1.000

Table-15 Correlation Coefficients amount Elements of the Original Analyses Data

	Cu	Pb	Zn	Ag	As	Mn	Ni	Co	Mo	Hg
Cu	1.000									
Pb	0.281	1.000						N:5,064		
Zn	0.199	0.091	1.000							
Ag	0.209	0.446	0.062	1.000						
As	0.107	0.236	-0.280	0.120	1.000					
Mn	0.207	0.092	0.623	-0.052	-0.017	1.000				
Ni	0.042	0.070	-0.255	0.041	0.250	0.111	1.000			
Co	0.219	0.015	0.668	0.001	-0.344	0.654	0.214	1.000		
Mo	0.056	0.117	-0.108	0.059	0.363	0.118	0.137	-0.116	1.000	
Hg	0.142	0.245	-0.029	0.252	0.272	-0.011	-0.073	-0.119	0.049	1.000

Of the cell average values, positive correlation coefficients more than 0.5 are observed among the following elements.

Pb-Ag, Zn-Mn, Zn-Co, Mn-Co

3-2-2-4 Areal distribution of the cell average values (Attached P1. 2-2 No. 1 - No. 10)

The cell average values of each element were classified into eleven ranks with the same range as that of Samar and plotted on a 1:1,000,000 scale map with the corresponding rank color.

The areal distribution zone of the anomalous cell averages are as follows (anomalous elements are shown in brackets). These localities are shown in Fig.-13.

A_L-1: Northern part of the area (At the central-eastern part of Biliran Is) (As, Hg)

A_L-2: Along the northwestern coast of the area (4 km SE of Villaba) (Cu, As, Mn, Ni, Mo, Hg).

A_L-3: Along the northeastern coast of the area (NE side of Tacloban) (Cu, Zn, Co)

A_L-4: Central-northern part of the area (24 km SW of Tacloban) (Zn, Mn, Co)

A_L-5: Central-eastern part of the area (15 km west of Dulag in the east coast) (Ni)

A_L-6: Southern part of the area (8 km north of Sogod) (Cu, Pb, Zn, As, Mn)

A_L-7: Southwestern part of the area (6 km north of Maasin in the south coast) (Cu, As, Ni, Hg)

A_L-8: Southeastern part of the area (northeastern coast of Panaon Is.) (Cu, Pb, Zn, Ag, As, Ni, Co, Hg)

On the basis of the above information, the following anomalous zones can be understood by considering the present knowledge on the geology, igneous activities and mineralization of the area.

(a) Central-eastern part of Biliran Island (A-1)

- This anomalous zone corresponds to the Biliran native sulphur mineral showing (33. Biliran) associated with Quaternary Volcanic fumarole. Emissions from the fumaroles could have led to the anomalies.

(b) Northwestern side of Tacloban (A-3)

This anomalous zone is associated with the Cretaceous pillow basalt hosted massive sulfide (41. Curajo, 48. Caibaan). It is inferred that the distribution of the pillow basalt suggests the extent of possible similar mineralization.

(c) 24 km SW of Tacloban (A-4)

This anomalous zone is located in the Miocene Central Highland Volcanics and is accompanied by nickeliferous vein type mineral showing (46. Antipolo). From the assemblage of anomalous elements, this zone is inferred to indicate the extent of similar mineralization.

(d) 4 km north of Sogod (A-6)

This anomalous zone is located in the Miocene Central Highland Volcanics and is associated with vein type mineral showing (23. Sogod). From the assemblage of anomalous elements, this could indicate a similar type of mineralization.

(e) The northeastern coast of Panaon Island

This anomalous zone occurs in the Miocene Central Highland Volcanics and exhibits gold-bearing vein type mineral showings (51. Anilao). From the assemblage of anomalous elements, this zone suggests a similar mineralization.

In addition to the above mentioned anomalous zones, concentrations of As, Mn, Ni, Mo anomalous cells are observed in the Miocene Bata and Tagnocot Formations at the northwestern part. However, the reason of these concentration and anomalies is not yet fully understood.

3-2-3 Univariate Analyses of Cell Average Data of Dinagat-Siargao

3-2-3-1 Basic statistical values

Basic statistical values of the cell average value for each element are shown in Table-16. Basic statistical values of the original analytical results are also shown in Table-17 for reference.

Regarding Pb, Ag over 95% cells show values below detection limit, therefor Pb, Ag are omitted in the statistical analysis.

Table-16 Basic Statistical Values of the Cell Average Data

	Cu (ppm)	Zn (ppm)	As (ppm)	Mn (ppm)	Ni (ppm)	Co (ppm)	Hg (ppb)	Cr (ppm)
M	42.26	99.06	1.72	1,434.17	1,023.24	132.60	39.52	817.02
M+1.0 σ	61.13	138.66	3.77	2,254.46	5,712.46	323.18	67.22	2,710.59
M+1.5 σ	73.52	164.05	5.59	2,826.58	13,497.23	504.55	87.67	4,937.20
M+2.0 σ	88.42	194.09	8.30	3,543.90	31,890.84	787.71	114.34	8,992.86
Maximum	184.00	378.00	120.26	4,200.00	7,250.00	610.00	231.06	8,800.00
Minimum	10.41	24.00	1.00	189.45	2.08	2.38	20.00	50.00
R. B. D.L.	0%	0%	0%	0%	0%	0%	53%	10%

R. B. D.L. : Ratio of cells below detection limit.

Table-17 Basic Statistical Values of the Original Analytical Results

	Cu (ppm)	Zn (ppm)	As (ppm)	Mn (ppm)	Ni (ppm)	Co (ppm)	Hg (ppb)	Cr (ppm)
M	40.98	98.20	1.74	1,470.35	1,227.77	147.08	40.16	893.52
M+1.0σ	65.26	141.94	4.42	2,472.66	7,036.52	373.70	79.23	2,970.23
M+1.5σ	83.35	170.65	7.04	3,206.55	16,845.31	595.68	111.29	5,414.42
M+2.0σ	103.92	205.17	11.22	4,158.24	40,327.38	949.52	156.32	9,869.93
Maximum	184.00	378.00	960.00	5,900.00	8,600.00	795.00	1,300.00	10,000.00
Minimum	8.00	18.00	1.00	60.00	1.50	1.50	20.00	50.00

Table-18 Details of Inflection Points of the Cumulative Frequency Curves for Elements and Cell Average Values

Element	Cu	Zn	As	Mn	Ni	Co	Hg	Cr
Cumulative Frequency	79%	83%	88%	96%	81%	95%	70%	94%
Cell averages	56 ppm	130 ppm	3 ppm	2,400 ppm	3,700 ppm	400 ppm	49 ppb	3,700 ppm

3-2-3-2 Histograms and cumulative frequency curves

Histograms and cumulative frequency curves showing the frequency distribution of the cell average values for each element were drawn (Appendix P1. 1-10). Inflection point of the curve was selected by the Lepeltier's method (1969) and its corresponding cell average value was regarded as the lowest anomalous value (threshold value). Inflection points for Pb and Ag could not be determined because over 95 percent of the cell contained Pb and Ag values below the detection limits. Details of the inflection point for each element are shown in Table-18.

3-2-3-3 Correlation Coefficients of Analysed Elements

Correlation coefficients among elements of cell averages are shown in Table-19. Correlation coefficients among elements of the original analytical results are also shown in Table-20.

Table-19 Correlating Coefficients of the Cell Average Data

	Cu	Pb	Zn	Ag	As	Mn	Ni	Co	Hg	Cr
Cu	1.000									
Pb	0.289	1.000								
Zn	0.448	-0.076	1.000							
Ag	0.121	0.279	0.017	1.000						
As	0.342	0.540	0.206	0.262	1.000					
Mn	-0.110	-0.361	0.533	-0.092	-0.107	1.000				
Ni	-0.417	-0.416	0.142	-0.092	-0.167	0.771	1.000			
Co	-0.304	-0.426	0.342	-0.085	-0.135	0.884	0.956	1.000		
Hg	0.239	0.294	0.388	0.137	0.494	0.428	0.355	0.424	1.000	
Cr	-0.267	-0.280	0.242	-0.064	-0.008	0.736	0.916	0.893	0.475	1.000

Of the cell average values, positive correlation coefficient of more than 0.5 are observed among the following elements:

Pb-As, Zn-Mn, Mn-Ni, Mn-Co, Mn-Cr, Ni-Co, Ni-Cr

Table-20 Correlation Coefficient of the Original Analysis

	Cu	Pb	Zn	Ag	As	Mn	Ni	Co	Hg	Cr
Cu	1.000									
Pb	0.250	1.000								
Zn	0.420	-0.069	1.000							
Ag	0.097	0.310	0.017	1.000						
As	0.291	0.568	0.177	0.198	1.000					
Mn	-0.019	-0.397	0.536	-0.115	-0.126	1.000				
Ni	-0.329	-0.443	0.178	-0.089	-0.201	0.710	1.000			
Co	-0.202	-0.444	0.391	-0.100	-0.165	0.873	0.931	1.000		
Hg	0.232	0.302	0.362	0.155	0.396	0.330	0.222	0.313	1.000	
Cr	-0.185	-0.299	0.314	-0.066	-0.038	0.663	0.885	0.854	0.349	1.000

3-2-3-4 Areal distribution of the cell average values (Attached P1. 2-1 Nos. 1 - 10)

The cell average values of each element were classified into eleven ranks as that of Samar and were plotted on a 1:1,000,000 scale map with the corresponding rank color.

The areal distribution zone of the anomalous cell averages are as follows (anomalous elements are shown in brackets). These localities are shown in Fig.-13.

Ap-1: Northern part of Dinagat Island. (Vicinity of Mt. Redondo) (Ni, Co)

Ap-2: West coast of Dinagat Island. (North side of Libjo) (As, Mn, Ni, Co, Hg, Cr)

Ap-3: East coast of Dinagat Island. (Vicinity of the mouth of San Jose River) (Ni, Co)

Ap-4: Southernmost part of Dinagat Island. (Vicinity of Mt. Gaboc) (Zn, As, Mn, Ni, Co, Hg)

Ap-5: Northern part of Bucas Grande Island. (Cu, Zn, As, Mn, Ni, Co, Hg)

Ap-6: Northern part of Masapelid Island. (Cu, Pb, As, Hg)

On the basis of the above information the following anomalous zones can be understood by taking into consideration the present

Table-21 Basic Statistical Values for the Moving Average Data in Samar

	Cu (ppm)	Zn(ppm)	As (ppm)	Mn (ppm)	Ni (ppm)	Co (ppm)	Cr (ppm)
M	38.19	75.22	1.72	720.01	77.48	26.56	1,649.10
M+1.0 σ	63.93	107.01	4.22	1,068.14	184.74	41.41	7,259.96
M+1.5 σ	82.72	127.64	6.62	1,300.99	285.27	51.72	15,232.72
M+2.0 σ	107.02	152.25	10.38	1,584.59	440.50	64.58	31,961.05
Maximum	128.96	248.48	26.50	1,776.50	1,066.60	83.86	45,738.00
Minimum	9.76	13.41	0.27	67.55	4.59	2.77	58.23
R. B. D.	0%	0%	14%	0%	0%	0.2%	2.8%

R. B. D. : Ratio of cells below detection limit.

knowledge on the geology, igneous activities and mineralization of the area.

(a) North side of Libjo (A_D-2)

This anomalous zone occurs in the peridotite massif and is associated with Cr mineral showing (Plate-(5) Velor). Recognized anomalies at the southern part seems to suggest a similar type of mineralization.

(b) Vicinity of Mt. Gaboc (A_D-4)

This anomalous zone occurs in the peridotite massif. This zone seems to concern Ni-laterite concentration similar to the Nonoc Mine deposit in the southern part.

(c) Northern part of Bucas Grande Island. (A_D-5)

This anomalous zone has no mineral showing, although orthomagmatic and vein type mineralizations can be expected on the basis of the anomalous elements assemblage.

(d) Northern part of Masapelid Island. (A_D-6)

This anomalous zone occurs in the Miocene Mabuhay andesite and is associated with gold-bearing quartz vein type mineral showing (15. Cangumod). This zone seems to indicate vein type Au-Ag mineralization on the basis of anomalous elements assemblage.

3-3 Moving Average Values

As stated in 3-1-1, the geochemical average of every nine cells in defined as the value of the central cell and this value is calculated for each movement in two kilometer steps. The gap-filling process for a blank cell is done in a way that when more than half of the immediately surrounding cells have effective values, the average of these cells is taken as the moving average value of the blank cell. This procedure was carried out twice.

The moving average values as stated above are suitable for finding general trends and geological changes of the source as each values represent the average of cells 6 km × 6 km in size around a particular cell.

3-3-1 Univariate Analyses of Moving Average Data of Samar

3-3-1-1 Basic statistical values

Basic statistical values for each element of the moving average values of Samar are shown in Table-21. All cells contained Pb, Ag and Hg values below detection limits, leading to their omission in the statistical analyses.

3-3-1-2 Histograms and cumulative frequency curves

Histogram and cumulative frequency curves of the moving average values were made for each element. Moving averages corresponding to inflection points of the cumulative frequency curves were regarded as the lowest anomalous values (threshold) by Lepeltier's method (1969).

Inflection points and threshold values for Ag, Pb and Hg could not be determined because 99 percent of the cells contained Ag, Pb and Hg values below detection limits. Details of the inflection points for each element are shown in Table-22.

Table-22 Details of Inflection Point of the Cumulative Frequency Curve

Element	Cu	Zn	As	Mn	Ni	Co	Cr
Cumulative Frequency	86%	81%	92%	90%	90%	93%	72%
Moving Averages	92 ppm	98 ppm	5.2 ppm	1,200 ppm	230 ppm	46 ppm	5,000 ppm

3-3-1-3 Areal distribution of the moving average values (Attached P1.2-2 Nos. 1 - 10)

The moving average values for each element were classified into eleven ranks and were plotted on a 1:1,000,000 scale map with the corresponding rank color.

Areal distribution of the anomalous moving average values of each element are as follows (anomalous elements are shown in brackets):

B_S-1: West side of Dolores in the east coast (As, Ni, Cr)

B_S-2: At 40 km west of Dolores in the east coast (Cu, Zn, Mn, Co)

B_S-3: At 12 km NNE of Catbalogan in the west coast (As, Hg)

B_S-4: At 13 km NE of Wright in the west coast (Zn, As, Mn)

B_S-5: West side of Borongan in the east coast (Cu, As, Mn, Ni, Co)

Table-23 Basic Statistical Values for the Moving Average Data in Leyte

	Cu (ppm)	Zn (ppm)	As (ppm)	Mn (ppm)	Ni (ppm)	Co (ppm)	Hg (ppb)
M	44.15	111.35	2.11	978.59	31.68	28.08	28.34
M+1.0σ	56.77	173.28	4.08	1,354.62	59.96	38.52	40.93
M+1.5σ	64.37	216.15	5.68	1,593.76	82.48	45.12	48.29
M+2.0σ	72.99	269.64	7.90	1,875.13	113.46	52.85	57.68
Maximum	185.87	343.00	14.58	2,548.90	331.17	64.07	323.83
Minimum	18.85	10.16	1.00	258.32	3.33	8.10	20.00
R. B. D.	0%	0%	0%	0%	0%	0%	85%

R. B. D. : Ratio of cells below detection limits.

B_S-6: West side of General MacArthur in the east coast (Zn, As, Mn, Ni, Cr)

B_S-7: North side of Balangiga in the south coast (Ni, Zn, Mn, Co)

B_S-8: At 20 km ESE of Basay in the western part of the south coast (Cu, Zn, Mn, Co)

These anomalous zones correspond to the anomalous zones defined by the cell average values except for the west side of Borongan. The concentration of anomalous elements is clearer than that defined by the cell average values.

3-3-2 Univariate Analyses of the Moving Averages Data of Leyte

3-3-2-1 Basic statistical values

Basic statistical values of moving averages data for each element in Leyte are shown in Table-23. All cells contained Pb, Ag and Hg values below detection limits, leading to their ommition in the statistical analysis.

3-3-2-2 Histograms and cumulative frequency curves

Histograms and cumulative frequency curves were made for each element. Moving averages values of corresponding to inflection points of the cumulative frequency curves were selected as the lowest anomalous values (threshold) following Lepeltier's method (1969).

Inflection points and threshold values for Pb, Ag and Mo could not be determined because over 95% of the cells contained Pb, Ag and Mo values below the detection limits. Details of the inflection point for each element are shown in Table-24.

3-3-2-3 Areal distribution of the moving average data (Attached P1.2-2 Nos. 1 - 10)

The moving average values for each element were classified into eleven ranks and were plotted on a 1:1,000,000 scale map with the corresponding rank color, similar to that of the cell average values.

Areal distribution of the anomalous moving average values of each element are as follows (anomalous elements are shown in brackets) (Pl.-13)

B_L-1: Central eastern part of Biliran Is. in the northern part (As, Hg)

Table-24 Details of Inflection Points of the Cumulative Frequency Curve

Element	Cu	Zn	As	Mn	Ni	Co	Hg
Cumulative Frequency	94%	92%	85%	92%	89%	79%	90%
Moving Averages	68 ppm	190 ppm	4.8 ppm	1,500 ppm	70 ppm	36 ppm	43 ppb

B_L-2: At 4 km SE of Villaba in the northeastern coast (Cu, As, Mn, Ni, Mo, Hg)

B_L-3: Northwest of Tacloban in the northeast coast (Cu, Mn, Ni, Co)

B_L-4: At 24 km Sw of Tacloban in the northeast coast (Zn, Mn, Co)

B_L-5: At 15 km west of Dulag in the east coast (Ni)

B_L-6: At 8 km north of Sogod in the southern part (Cu, Pb, Zn, Mn)

B_L-7: At 6 km north of Maasin in the southwest coast (Cu, Ni, Hg)

B_L-8: Northeast coast of Panaon Is. in the southeastern part (Cu, Pb, Zn, Ag, As, Co)

All these anomalous zones overlap the anomalous zones defined by the cell average values. However, the concentration of anomalous cells is clearer than that of cell average values. In terms of the anomalous elements as compared to those present in the cell average value defined anomalies, Zn is lacking and Mn, Ni are added at B_L-3. Arsenic is lacking at B_L-6 and B_L-7 and Ni is lacking at B_L-8. The above mentioned anomalous zones can be understood by taking into consideration the present knowledge on the geology, igneous activities and mineralizations of the area.

(a) Central-eastern part of Biliran Is. (B_L-1).

(b) Northwest side of Tacloban along the northeast coast (B_L-3).

(c) 24 km SW of Tacloban (B_L-4).

(d) 8 km north of Sogod in southern part (B_L-6).

(e) Northeast coast of Panaon Is. (B_L-8).

In addition to these zone, concentration of Cu, As, Mn and Ni anomalous cells are observed in the northwestern part of the area associated with the Miocene Bata and Tagnocot Formations. However, the reason for such anomalous concentrations is not yet clear.

3-3-3 Univariate Analyses of Moving Average Data of Dinagat-Siargao

3-3-3-1 Basic statistical values

Basic statistical values of moving average data of Dinagat-Siargao are shown on Table-25. The Pb and Ag content of most of the samples are below the detection limit so these were omitted from the analysis.

3-3-3-2 Histograms and cumulative frequency curves

Histograms and cumulative frequency curves of moving average values were made for each element. Moving average values corresponding to inflection points of the cumulative frequency curve was selected as the lowest anomalous values (threshold) following Lepeltier's method (1969). Inflection points and threshold values for Ag and Pb could not be determined because 99 percent of the samples have Ag and Pb values below the detection limits. Details of inflection points for each element are shown in Table-26.

3-3-3-3 Areal distribution of moving average data in Dinagat-Siargao (Attached P1.2-2 Nos. 1 - 10)

Moving average values for each element are classified into eleven ranks similar to that of cell average values and are plotted in a 1 : 1,000,000 scale map with the corresponding rank color.

Concentration zone of anomalous cells are as follows (anomalous elements are shown in brackets) (Pl.-13):

B_D-1: Vicinity of Mt. Redondo in northern Dinagat Is. (Mn, Ni, Co)

B_D-2: North side of Libjo in the west coast of Dinagat Is. (As, Mn, Ni, Co, Hg, Cr)

B_D-3: Vicinity of the mouth of San Jose River in east coast Dinagat Is. (Ni, Co, Cr)

B_D-4: Vicinity of Mt. Gaboc in southern Dinagat Is. (Zn, As, Mn, Ni, Co, Hg, Cr)

B_D-5: Northern part of Bucas Grande Is. (Cu, Zn, As, Mn, Ni, Co, Hg, Cr)

B_D-6: Northern part of Masapelid Is. (Cu, Pb, As, Hg)

All these anomalous zones overlap the anomalous zones defined by cell averages. The concentration of anomalous cells is clearer than that of the cell averages. In term of the anomalous elements, Mn is added to B_D-1 zone while Cr is added to B_D-3 and B_D-5 zones. The following four anomalous zones can be understood by taking into consideration the geology, igneous activities and mineralizations of the area. These zones are basically similar to that of the cell average data.

(a) North side of Libjo in the west coast of Dinagat Is. (B_D-2)

(b) Vicinity of Mt. Gaboc in the southern part of Dinagat Is. (B_D-4)

(c) Northern part of Bucas Grande (B_D-5)

(d) Northern part of Masapelid Is. (B_D-6)

3-4 Univariate Analyses of High-pass Filter Valuers

As stated in 3-1-1, the positive difference between the cell average and the corresponding moving average values is defined as the high-pass filter value. This indicates the extent of the deviation of the individual cell averages from the filtered moving averages. Calculating the difference between the two values offsets the background value, and thus the high-pass filter values indicate anomalous zones derived from such added factors as mineralization and secondary enrichment. These values provide guidelines regarding the locality, strength and priority of the geochemical anomalous zones.

Table-25 Basic Statistical Values of Moving Averages of Dinagat-Siargao

	Cu (ppm)	Zn (ppm)	As (ppm)	Mn (ppm)	Ni (ppm)	Co (ppm)	Hg (ppb)	Cr (ppm)
M	41.18	97.62	1.65	1,460.83	1,203.10	142.14	39.44	897.61
M+1.0σ	52.62	124.20	2.73	2,033.10	4,853.34	288.09	57.03	2,349.31
M+1.5σ	59.48	140.16	3.51	2,398.49	9,747.89	410.15	68.58	3,800.71
M+2.0σ	67.24	158.03	4.52	2,829.55	19,578.53	583.92	82.47	6,148.79
Maximum	92.71	203.21	25.37	3,187.10	5,453.20	411.72	109.95	6,644.30
Minimum	23.52	56.28	1.00	426.26	8.00	10.44	20.00	55.92
R. M. D.	0 %	0 %	0 %	0 %	0 %	0 %	53 %	7 %

R. M. D. : Ratio of cells below detection limit.

Table-26 Details of Inflection Points of the Cumulative Frequency Curves

Element	Cu	Zn	As	Mn	Ni	Co	Hg	Cr
Cumulative frequency	94%	85%	93%	80%	93%	80%	78%	93%
Moving averages	62ppm	120ppm	3 ppm	1,950 ppm	7,000 ppm	230ppm	52 ppb	3,000ppm

Table-27 Basic Statistical Values for each Element of the High-pass Filter Data

	Cu (ppm)	Pb (ppm)	Zn (ppm)	As (ppm)	Mn (ppm)	Ni (ppm)	Co (ppm)	Hg (ppb)	Cr (ppm)
M	3.12	1.34	5.35	0.64	61.90	9.72	1.96	2.75	439.07
M+1.0σ	12.57	5.04	25.10	2.21	291.23	63.53	7.46	12.42	6,101.88
M+1.5σ	25.23	9.79	54.37	4.12	631.67	162.41	14.55	27.66	22,747.28
M+2.0σ	50.67	19.01	117.81	7.69	1,370.07	415.21	28.36	56.20	84,799.83
Maximum	47.24	6.13	125.10	17.60	1,903.80	984.24	32.94	90.95	86,903.00
Minimum	0.12	0.10	0.10	0.10	0.13	0.11	0.10	0.16	0.11

Table-28 Details of Inflection Points for each Element on the Cumulative Frequency Curves

Element	Cu	Zn	As	Mn	Ni	Co	Hg	Cr
Cumulative Frequency	89%	86%	78%	95%	90%	87%	88%	91%
High-pass filter value	19 ppm	38 ppm	1.8 ppm	410 ppm	100 ppm	10 ppm	19 ppb	11,000 ppm

3-4-1 Univariate Analyses of High-pass Filter Data of Samar

3-4-1-1 Basic statistical values

Basic statistical values for each element of the high-pass filter data are shown in Table-27. No cell contained effective Ag value, thus Ag values were omitted from the statistical analyses.

3-4-1-2 Histograms and cumulative frequency curves

Histograms and cumulative frequency curves of the high-pass filter values for each element were prepared. Inflection point of the curve was selected following Lepeltier's method (1969) and its corresponding high-pass filter value was regarded as the lowest anomaly value (threshold value). There are no threshold value for Pb and Ag since more than 98 percent of the cells contained no effective Pb and Ag values. Details of the inflection points for the elements are shown in Table-28.

3-4-1-3 Areal distribution of high-pass filter anomalous values (Attached P1.2-3 Nos. 1 - 9)

Each anomalous value was classified based on the following formula for each element and was plotted on a 1 : 1,000,000 scale map with the corresponding rank color. All the threshold values selected were more than M+1.0σ.

Classified Rank of High-pass filter Anomalous Value

Classified Formula	Color	Rank
M+2.0σ ≦ Z <	Red	A
M+1.5σ ≦ Z < M+2.0σ	Yellow	B
M+1.0σ ≦ Z < M+1.5σ	Blue	C

The following zones of anomalous high-pass filter values are related to the anomalous zones defined by the cell averages and are considered important (anomalous elements are shown in brackets) (Pl.-13):

C_S-1: West side of Dolores in the east coast (Cu, Zn, As, Mn, Ni, Hg)

C_S-2: 40 km west of Dolores in the east coast (Cu, Zn, Mn, Co, Hg)

C_S-3: 12 km NNE of Catbalogan in the west coast (As, Mn, Co, Hg)

C_S-4: 13 km NE of Wright in the west coast (Cu, Pb, Zn, As, Mn, Co, Cr)

C_S-5: West side of Borongan in the east coast (Cu, As, Mn, Cr)

C_S-6: West side of General MacArthur in the southeast coast (As, Mn, Ni, Co, Cr)

C_S-7: North side of Balangiga in the south coast (Ni, Co, Hg, Cr)

These anomalous zones except for C_S-5 overlap the anomalous zones defined by the Cell average data. When compared with results of the cell average data, additional elements found at C_S-1 are Cu, Zn and Mn while Cr is lacking; at C_S-4 zone, Cu, Pb, Zn, Co, Cr are added while Hg is lacking and at C_S-6 zone, Mn is added while Zn is lacking.

The relationship between these zones and the geological setting is unclear, since the geological survey work is still unfinished.

3-4-2 Univariate Analyses of High-pass Filter Data of Leyte

3-4-2-1 Basic statistical values

Basic statistical values for each element of high-pass filter data are shown in Table-29.

Over 95 percent of the samples have Pb, Ag and Mo values below the detection limits, so these elements are omitted from the analysis.

3-4-2-2 Histograms and cumulative frequency curves

Histograms and cumulative frequency curves of the high-pass filter data for each element were prepared. Inflection point of the curve was selected following the Lepeltier's method (1969) and its corresponding high-pass filter value was regarded as the lowest anomalous value (threshold value). There are no threshold values

Table 29 Basic Statistical Values for the High-pass Filter Data of Leyte

	Cu (ppm)	Zn (ppm)	As (ppm)	Mn (ppm)	Ni (ppm)	Co (ppm)	Hg (ppb)
M	3.49	11.19	0.82	83.39	4.02	2.64	6.64
M+1.0 σ	12.87	46.58	2.73	355.55	21.01	8.94	34.27
M+1.5 σ	24.72	95.05	4.98	734.18	48.05	16.46	77.83
M+2.0 σ	47.46	193.95	9.09	1,516.01	109.91	30.30	176.77
Maximum	3,914.10	262.50	68.42	2,868.00	1,255.20	51.83	4,728.20
Minimum	0.10	0.11	0.10	0.26	0.10	0.10	0.10

Table-30 Details of Inflection Points for the Cumulative Frequency Curve of Leyte

Element	Cu	Zn	As	Mn	Ni	Co	Hg
Cumulative Frequency	93%	91%	89%	94%	91%	92%	93%
High-pass Filter Value	18 ppm	66 ppm	3.6 ppm	500 ppm	31 ppm	12 ppm	50 ppb

for Pb, Ag and Mo as more than 95 percent of the cells contain no effective Pb, Ag and Mo values.

Details of the inflection points for the elements are shown in Table-30.

3-4-2-3 Areal distribution of high-pass filter anomalous value in Leyte (Attached P1.2-3 Nos. 1 - 9)

Each anomalous value was classified into three ranks based on its cumulative frequency, and plotted on a 1 : 1,000,000 scale map with the corresponding rank color. This is similar to what has been done to the Samar data. Concentration zone of anomalous cells are as follows (Anomalous elements are shown in brackets) (Pl.-13):

C_L-1: Central east part of Biliran Is. (As, Mn, Co, Hg, Mo)

C_L-2: 4 km SE of Villaba in the northwest coast (Mo)

C_L-3: Northwest side of Tacloban in the northeast coast (Cu, Zn, Ni, Co)

C_L-4: 24 km SW of Tacloban (Mn, Co)

C_L-5: 8 km north of Sogod in the southern part (Cu, Pb, Zn, As, Mn, Ni, Co, Hg)

C_L-6: 8 km north of Maasin in the southwestern coast (Cu, As, Mn, Ni, Co, Hg)

C_L-7: Northeast coast of Panaon Is. (Cu, Pb, Zn, Ag, As, Ni, Co, Mo, Hg)

In comparing these zones with the cell average anomalous zone, additional elements are Mn, Co, Mo, in C_L-1 zone, Ni in C_L-3 zone, Ni, Co, Hg in C_L-5 zone, Mn, Co in C_L-6 zone and Mo in C_L-7 zone. Cu, As, Mn, Ni, Hg are absent in C_L-2 zone while Cu is lacking in C_L-4 zone. The A_L-5 anomalous zone (15 km of Dulag in the east coast) is not recognized on the high-pass filter analysis.

Of the above anomalous zones, the following five anomalous zones which are similar to the anomalous zones defined by the cell average analysis can be understood by taking into consideration the present knowledge on the geology, igneous activities and mineralizations of the area.

(a) Central east part of Biliran Is. (C_L-1)

(b) Northwest side of Tacloban in the northeast coast (C_L-3)

(c) 24 km SW of Tacloban (C_L-4)

(d) 8 km north of Sogod in the southern part (C_L-5)

(e) Northeast coast of Panaon Is. (C_L-7)

3-4-3 Univariate Analyses of High-Pass Filter Data of Dinagat-Siargao

3-4-3-1 Basic statistical values

Basic statistical values for each element of the high-pass filter data in are shown in Table-31. Only four cells for Pb and two cells for Ag contain effective values. These are omitted from the analyses.

3-4-3-2 Histograms and cumulative frequency curves

Histograms and cumulative frequency curves of the high-pass filter data for each element were prepared. Inflection point of the

Table-31 Basic Statistical Values for each Element of the High-pass Filter Values of Dinagat-Siargao

	Cu (ppm)	Zn (ppm)	As (ppm)	Mn (ppm)	Ni (ppm)	Co (ppm)	Hg (ppb)	Cr (ppm)
M	4.35	7.17	0.82	160.79	357.87	24.16	7.87	222.74
M+1.0 σ	19.37	29.49	3.59	722.55	2,125.20	115.93	31.05	941.73
M+1.5 σ	40.88	59.82	7.48	1,531.71	5,178.90	253.96	61.73	1,936.36
M+2.0 σ	86.25	121.34	15.61	3,247.03	12,620.48	556.33	122.70	3,981.51
Maximum	137.18	73.12	94.89	1,985.50	3,833.80	320.81	176.38	3,465.60
Minimum	0.12	0.12	0.10	1.58	1.30	0.19	0.16	5.76

Table-32 Details of Inflection Points of the Cumulative Frequency Curves on High-pass Filter values of Dinagat-Siargao

Element	Cu	Zn	As	Mn	Ni	Co	Hg	Co
Cumulative Frequency	92%	78%	90%	96%	99%	95%	93%	91%
High-pass Filter Value	29 ppm	21 ppm	5.1 ppm	990 ppm	3,100 ppm	180 ppm	42 ppb	1,300 ppm

curve was selected following the Lepeltier's method (1969) and its corresponding high-pass filter value was regarded as the lowest anomalous value (threshold value). Threshold values for Pb and Ag could not be selected as almost all cells contained no effective values.

Details of the inflection points for the elements are shown in Table-32.

3-4-3-3 Areal distribution of high-pass filter anomalous value in Dinagat-Siargao (Attached P1.2-3 Nos. 1 - 9)

Each anomalous value was classified into three ranks similar to what has been done to the Samar and Leyte data and was plotted on a 1 : 1,000,000 scale map with the corresponding rank color.

The following zones of anomalous high-pass filter values are related to the anomalous zones defined by the cell averages and are considered important (anomalous elements are shown in brackets) (Pl.-13):

C_D-1: Vicinity of Mt. Redondo in the northern part of Dinagat Is. (Cu, Zn, Ni, Co)

C_D-2: North side of Libjo in the west coast of Dinagat Is. (Zn, Mn, Ni, Co, Hg, Cr)

C_D-3: At the mouth of San Jose River in the East coast of Dinagat Is. (Cu, Zn, Co, Cr)

C_D-4: Vicinity of Mt. Gaboc in the southern part of Dinagat Is. (Mn, Ni, Co, Hg, Cr)

C_D-5: Northern part of Bucas Grande Is. (Zn, Mn, Ni, Co, Hg, Cr)

C_D-6: Northern part of Masapelid Is. (Cu, Pb, Zn, Zn, As, Mn, Hg)

Comparing these results to the cell average values, additional anomalous elements are Cu and Zn for C_D-1 zone, Zn for C_D-2 zone, Cr for C_D-5 zone and Zn and Mn for C_D-6 zone. Elements that are lacking are As for C_D-2 zone, Ni for C_D-3 zone Zn and As for C_D-4 zone and Cu and As for C_D-5 zone.

Of the above anomalous zones, the following four zones are considered to be related to mineralization based on their geological settings.

(a) North side of Libjo in the west coast of Dinagat Is. (C_D-2)

(b) Vicinity of Mt. Gaboc in the southern part of Dinagat Is. (C_D-4)

(c) Northern part of Bucas Grande Is. (C_D-5)

(d) Northern part of Masapelid Is. (C_D-6)

3-5 Factor Analyses of Cell Average Values

Factor analysis was carried out on the Leyte and Dinagat-Siargao data using Varimax rotation method. As for Samar, since the geological survey was suspended and the geochemical sample density is not uniform, factor analysis was not carried out.

Eigenvalues are calculated for cases which have diagonal factor; 1.

3-5-1 Factor Analyses of Cell Average Data of Leyte

3-5-1-1 Extraction of factors

Correlation matrix and eigenvalue (λ) taken from normalization and interpretation of the cell average values for elements are shown in Table-33 and Table-34.

Table-33 Correlation Matrix of Leyte Data

	Cu	Pb	Zn	Ag	As	Mn	Ni	Co	Mo	Hg
Cu	1.000									
Pb	0.346	1.000								
Zn	0.213	0.083	1.000							
Ag	0.329	0.654	0.052	1.000						
As	0.057	0.237	-0.319	0.136	1.000					
Mn	0.216	0.074	0.615	-0.068	0.005	1.000				
Ni	0.030	0.111	-0.340	0.091	0.305	0.052	1.000			
Co	0.265	0.029	0.660	0.014	-0.390	0.646	0.134	1.000		
Mo	0.057	0.098	-0.152	0.021	0.458	0.168	0.199	-0.134	1.000	
Hg	0.205	0.376	0.017	0.417	0.254	0.001	-0.089	-0.091	0.017	1.000

Table-34 Eigenvalues and Cumulative Proportion of Variance of Leyte Data

Factor	No. 1	No. 2	No. 3	No. 4	No. 5	No. 6	No. 7
Eigenvalue (λ) (Diagonal Factor; 1)	2.551	2.356	1.525	1.021	0.715	0.641	0.469
Cumulative Proportion of variance	0.255	0.493	0.645	0.747	0.819	0.889	0.930

It can be seen from Table-34 that the eigenvalues in decreasing order are $\lambda_1 = 2.551$, $\lambda_2 = 2.356$ - - - and if those over 1 are taken, 4 factors will be considered. However, as λ_5 and λ_6 are also large and the cumulative proportion of total variance reaches 81 percent up to λ_5, the 5 factors are adopted.

3-5-1-2 Interpretation of each factor

Adopting the five factors and diagonal factor; 1, the left half of Table-35, shows the factor loadings obtained which were processed by the main analysis. The right half of Table-35, on the other hand, shows the factor loadings after processing using the Varimax rotation method.

Table-35 Factor Loadings

Before Rotation						After Rotation					
Factor	No.1	No.2	No.3	No.4	No.5	Factor	No.1	No.2	No.3	No.4	No.5
Cu	0.387	0.524	-0.033	0.099	0.664	Cu	0.181	0.251	0.070	-0.031	0.880
Pb	0.119	0.805	-0.191	0.124	-0.048	Pb	0.050	0.780	0.085	0.136	0.282
Zn	0.883	-0.032	-0.054	-0.254	-0.079	Zn	0.827	0.072	-0.202	-0.339	0.098
Ag	0.081	0.764	-0.352	0.218	-0.050	Ag	-0.053	0.813	-0.077	0.128	0.281
As	-0.462	0.539	0.428	-0.276	-0.094	As	-0.199	0.275	0.788	0.169	-0.095
Mn	0.737	0.108	0.493	-0.213	-0.163	Mn	0.902	-0.020	0.235	0.033	0.027
Ni	-0.191	0.264	0.589	0.672	-0.203	Ni	-0.006	0.038	0.180	0.955	-0.016
Co	0.871	-0.040	0.228	0.258	-0.112	Co	0.853	-0.037	-0.291	0.225	0.163
Mo	-0.220	0.336	0.647	-0.382	0.205	Mo	0.036	-0.076	0.859	0.068	0.139
Hg	-0.007	0.619	-0.340	-0.312	-0.364	Hg	0.013	0.783	0.157	-0.244	-0.179

Interpretation of each factor are as follows.

(a) Factor No. 1

Factor loadings before rotation except for As, Ni, Mo and Hg are positive with Zn, Mn and Co showing high values. These values after rotation exhibit similar tendencies as well. This factor seems to be related to a Zn-Mn-Co assemblage that could indicate base metal mineralization in the serpentinite.

(b) Factor No. 2

Factor loadings before rotation except for Zn and Co are positive with Pb, Ag and Hg showing high values. These values after rotation exhibit similar tendencies as well. This factor seems to indicate Pb-Ag-Hg assemblage and suggests the presence of gold-silver bearing vein type mineralization.

(c) Factor No. 3

Factor loadings before rotation except for Cu, Pb, Zn, Ag and Hg are positive, especially Ni and Mo which show high values. After rotation, factor loading values except for Zn, Ag and Co are positive, with As and Mo showing high values. This factor seems to indicate Mo mineralization and possible concentration of Ni and As in the country rocks.

(d) Factor No. 4

Factor loadings before rotation except for Zn, As, Mn, Mo and Hg are positive, especially Ni which shows a high value. Factor loadings of Cu, Zn and Hg after rotation are negative while the other elements are positive with Ni showing a high value. This factor indicates Ni mineralization.

(e) Factor No. 5

Factor loadings before rotation show Cu and Mo positive values while the other elements show negative values, Cu shows a high value. After rotation, factor loadings of Cu is still positive and high. This factor seems to be related to copper mineralization.

3-5-1-3 Classification of factor score

Factor score of each cell was calculated by multiplying the cell average value by the factor score coefficient and summarizing them for every cell. After the statistical procedure was done, these factor scores were classified into the following eight ranks and were plotted on a 1 : 1,000,000 scale map (Attached P1.2-4 Nos. 1 - 5)

Rank	Frequency	Rank	Frequency
A	90%≦Z<100%	E	30%≦Z<50%
B	80%≦Z<90%	F	20%≦Z<30%
C	70%≦Z<80%	G	10%≦Z<20%
D	50%≦Z<70%	H	0%≦Z<10%

3-5-1-4 Distribution of the geochemical anomalies (factor scores)

The attached P1.2-4 Nos. 1 - 5 show the areal distribution of the factor scores. The areas of concentration of high score are as follows. (Fig. 14)

(A) Factor No. 1 (Closely related to Zn, Mn and Co)

D-1-1: Concentration of A and B rank cells in the area of the Miocene Central Highland Volcanics 24 km SW of Tacloban.

D-1-2: Concentration of B, C and D rank cells in the area of the Miocene Central Highland Volcanics 15 km west of Dulag.

D-1-3: Concentration of A and B rank cells in the area of the Miocene Central Highland Volcanics 8 km north of Sogod.

D-1-4: Concentration of A, B and C rank cells in the area of the Miocene Central Highland Volcanics at the northeast coast of Panaon Is.

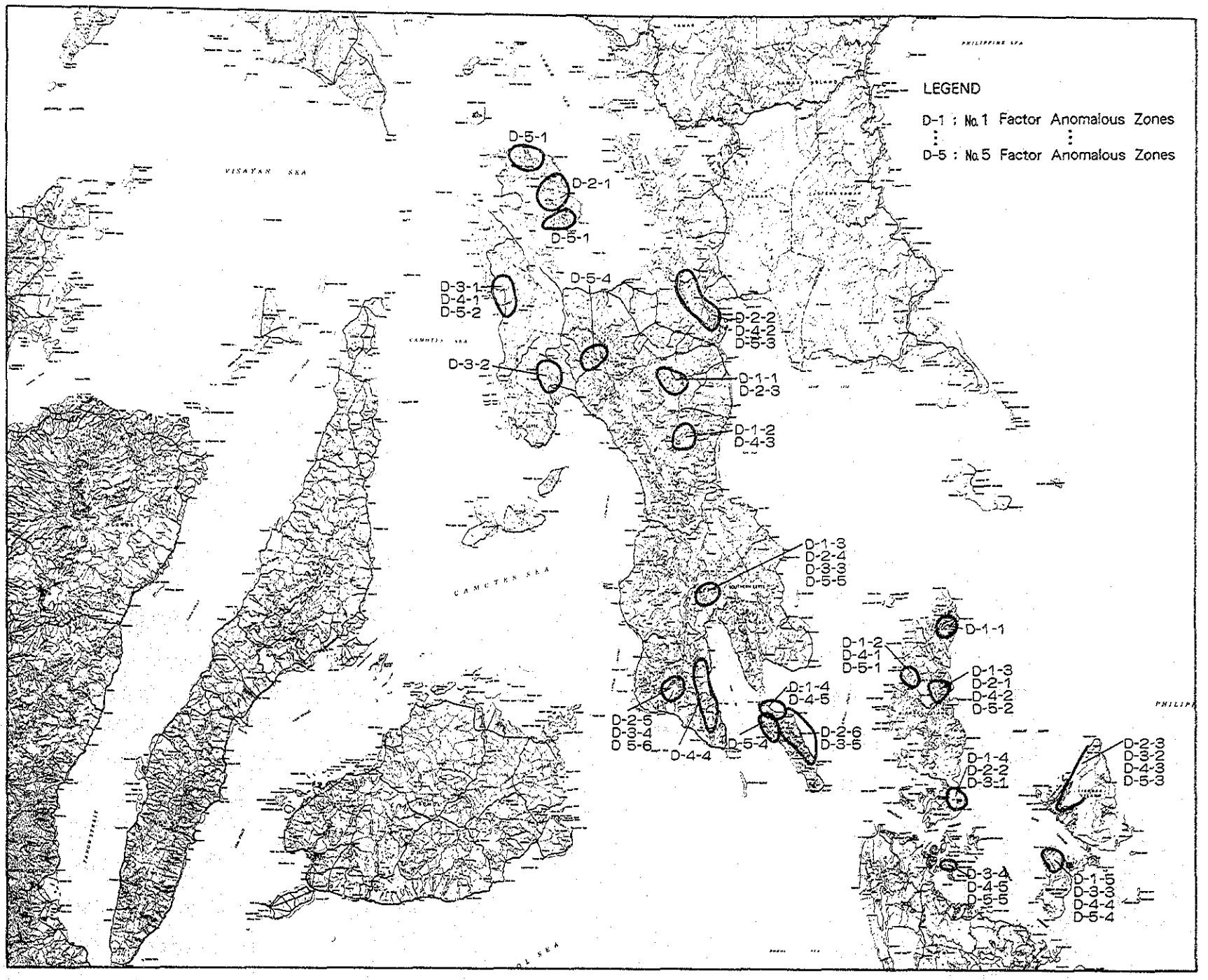

Fig. -14 Anomalous Zones of Factor Analyses in Leyte, Dinagat and Siargao Area

(B) Factor No. 2 (Closely related to Pb, Ag and Hg)

D-2-1: Concentration of A, B and C rank cells in the area of the Quaternary Volcanics at the eastern part of Biliran Is..

D-2-2: Concentration of G and H rank cells in the area of Cretaceous pillow basalts at the northwest side of Tacloban (negative anomaly).

D-2-3: Concentration of B and C rank cells in the area of the Miocene Central Highland Volcanics 24 km SW of Tacloban.

D-2-4: Concentration of A and B rank cells in the area of the Miocene Central Highland Volcanics 8 km north of Sogod.

D-2-5: Concentration of A and B rank cells in the area of the Miocene limestone 20 km north of Maasin.

D-2-6: Concentration of A and B rank cells in the area of the Miocene Central Highland Volcanics at the northeast coast of Panaon Is.

(C) Factor No. 3 (Closely related to As, Ni and Mo)

D-3-1: Concentration of A and B rank cells in the area of Miocene sedimentary rocks at the vicinity of Villaba in the Northwest coast.

D-3-2: Concentration of A and B rank cells in the area of the Miocene Central Highland Volcanics 16 km NNE of Ormoc.

D-3-3: Concentration of A and B rank cells in the area of the Miocene Central Highland Volcanics 8 km north of Sogod.

D-3-4: Concentration of A and B rank cells in the area of Miocene limestone 20 km north of Maasin.

D-3-5: Concentration of A, B and C rank cells in the area of the Miocene Central Highland Volcanics at the northeast coast of Panaon Is..

(D) Factor No. 4 (Closely related to Ni)

D-4-1: Concentration of A, B and C rank cells in the area of Miocene tuff and sandstone at the vicinity of Villaba in the northwest coast.

D-4-2: Concentration of A and B rank cells in the area of Cretaceous ultramafic rocks at the northwest side of Tacloban.

D-4-3: Concentration of A and B rank cells in the area of the Miocene Central Highland Volcanics 15 km west of Dulag.